โครงการการเรียนการสอนเพื่อเสริมประสบการณ์

การวิเคราะห์แฟร็กทัลของรอยเลื่อน ในภูมิภาคเอเชียตะวันออกเฉียงใต้แผ่นดินใหญ่

โดย

นายธรรมปพน สรรพอุดม
เลขประจำตัวนิสิต 5932712723

โครงการนี้เป็นส่วนหนึ่งของการศึกษาระดับปริญญาตรี
ภาควิชาธรณีวิทยา คณะวิทยาศาสตร์ จุฬาลงกรณ์มหาวิทยาลัย
ปีการศึกษา 2562

การวิเคราะห์แฟร็กทัลของรอยเลื่อนในภูมิภาคเอเชียตะวันออกเฉียงใต้แผ่นดินใหญ่

นายธรรมปพน สรรพอุดม

โครงงานนี้เป็นส่วนหนึ่งของการศึกษาตามหลักสูตรวิทยาศาสตรบัณฑิต
ภาควิชาธรณีวิทยา คณะวิทยาศาสตร์ จุฬาลงกรณ์มหาวิทยาลัย
ปีการศึกษา 2562

FRACTAL ANALYSIS OF FAULTS IN THE MAINLAND SOUTHEAST ASIA

MISTER THAMPAPHON SUNPA-UDOM

A Project Submitted in Partial Fulfillment of the Requirements

for the Degree of Bachelor of Science Program in Geology

Department of Geology, Faculty of Science, Chulalongkorn University

Academic Year 2019

หัวข้อโครงงาน	การวิเคราะห์แฟร็กทัลของรอยเลื่อนในภูมิภาคเอเชียตะวันออกเฉียงใต้แผ่นดินใหญ่
โดย	นายธรรมปพน สรรพอุดม
สาขาวิชา	ธรณีวิทยา
อาจารย์ที่ปรึกษาโครงการหลัก	รองศาสตราจารย์ ดร.สันติ ภัยหลบลี้

วันที่ส่ง.....

วันที่อนุมัติ.....

.....

อาจารย์ที่ปรึกษาโครงการหลัก

(รองศาสตราจารย์ ดร.สันติ ภัยหลบลี้)

Project Title	FRACTAL ANALYSIS OF FAULTS IN THE MAINLAND SOUTHEAST ASIA
By	Mister Thampaphon Sunpa-udom
Field of Study	Geology
Project Advisor	Associate Professor Dr. Santi Pailoplee

Submitted date.....

Approval date.....

.....

Project Advisor

(Associate Professor Dr. Santi Pailoplee)

ธรรมปพน สรรพอุดม : การวิเคราะห์แฟร็กทัลของรอยเลื่อนในภูมิภาคเอเชียตะวันออกเฉียงใต้แผ่นดินใหญ่. (FRACTAL ANALYSIS OF FAULTS IN THE MAINLAND SOUTHEAST ASIA) อ.ที่ปรึกษาโครงงานหลัก : รองศาสตราจารย์ ดร.สันติ ภัยหลบลี้, 45 หน้า.

บทคัดย่อ

ปรากฏการณ์แผ่นดินไหวเป็นผลมาจากกระบวนการแปรสัณฐานซึ่งอาจก่อให้เกิดร่องรอยการปริแตกของพื้นผิวในรูปของรอยเลื่อน โดยรอยเลื่อนเหล่านี้มีรูปร่างที่ขรุขระ ไม่เป็นระเบียบ ซึ่งค่าของมิติแฟร็กทัลสามารถถูกนำมาใช้ในการอธิบายความไม่เป็นระเบียบนี้ได้ การศึกษานี้จึงสนใจการวิเคราะห์แฟร็กทัลด้วยวิธีบอกซ์เคาน์ติ้ง (Box Counting) เพื่อใช้คำนวณหาค่ามิติแฟร็กทัลจากรูปร่างของรอยเลื่อนในภูมิภาคเอเชียตะวันออกเฉียงใต้แผ่นดินใหญ่ โดยการแบ่งพื้นที่ศึกษาออกเป็นช่องเล็ก ๆ ขนาดเท่า ๆ กัน แล้วคำนวณค่ามิติแฟร็กทัลจากรูปร่างของรอยเลื่อนในแต่ละช่อง ผลการคำนวณพบว่ามิติแฟร็กทัลมีค่าอยู่ในช่วง 0.831–1.204 สำหรับการแบ่งเป็นช่องละ 1°×1° มีค่าอยู่ในช่วง 0.806–1.253 สำหรับการแบ่งเป็นช่องละ 0.5°×0.5° และมีค่าอยู่ในช่วง 0.802–1.229 สำหรับการแบ่งเป็นช่องละ 0.25°×0.25° โดยสังเกตได้ว่าพื้นที่ที่มิติแฟร็กทัลมีค่าสูงนั้นคือพื้นที่ที่รอยเลื่อนมีรูปร่างซับซ้อนและไม่เป็นระเบียบ นอกจากการแบ่งพื้นที่ศึกษาเป็นช่องขนาดเท่า ๆ กันแล้ว ยังแบ่งตามเขตการเกิดแผ่นดินไหวของพื้นที่ศึกษาด้วย พบว่าเขตที่มิติแฟร็กทัลมีค่าต่ำที่สุดนั้นคือเขตแอ่งอันดามัน มีค่า 0.906 และเขตที่มิติแฟร็กทัลมีค่าสูงที่สุดนั้นคือเขตตะวันตกของประเทศไทย มีค่า 1.194 นอกจากนี้ ฐานข้อมูลแผ่นดินไหวที่ได้จากเครื่องมือตรวจวัดได้ถูกนำมาใช้เพื่อคำนวณตัวแปรด้านพฤติกรรมแผ่นดินไหวในพื้นที่ศึกษาเพื่อนำมาใช้เทียบสัมพันธ์กับค่ามิติแฟร็กทัล ทั้งนี้ ไม่พบความสัมพันธ์ระหว่างค่ามิติแฟร็กทัลกับตัวแปรด้านพฤติกรรมแผ่นดินไหวอย่างมีนัยสำคัญทางสถิติ

ภาควิชา ธรณีวิทยา ลายมือชื่อนิสิต .....

สาขาวิชา ธรณีวิทยา ลายมือชื่ออ.ที่ปรึกษาหลัก .....

ปีการศึกษา 2562

5932712723 : MAJOR GEOLOGY

KEYWORDS : FRACTAL ANALYSIS / FAULT GEOMETRY / MAINLAND SOUTHEAST ASIA

THAMPAPHON SUNPA-UDOM : FRACTAL ANALYSIS OF FAULTS IN THE MAINLAND SOUTHEAST ASIA. ADVISOR : ASSOCIATE PROFESSOR DR.SANTI PAILOPLEE, Ph.D., 45 pp.

ABSTRACT

Seismic activity of a region is a result of an underlying tectonic movement that could leave traces of ruptures on the surface in a form of faults. These fault lines exhibit irregular geometry that could be described as fractal dimension. This study focuses on fractal analysis using box-counting method for fault lines in the mainland Southeast Asia and calculates the fractal dimension values. The calculation is executed for three different grid spacings dividing the study area. The value of fractal dimension ranges from 0.831 to 1.204 in 1°×1° grid size, from 0.806 to 1.253 in 0.5°×0.5° grid size, and from 0.802 to 1.229 in 0.25°×0.25° grid size. Segments of fault associate with significantly high fractal dimension are observably complex and irregular on the regional scale. Besides equally divided into grids, the fault lines are extracted according to seismic source zones of the study area resulting in the value of fractal dimension ranges from the lowest of 0.906 in Andaman Basin to the highest of 1.194 in Western Thailand. Earthquake record data is also utilized to calculate seismicity parameters of the study area and be correlated to the fractal dimension. However, there is no significant relationship between fractal dimension to any of the seismicity parameters.

Department : Geology Student's Signature.....

Field of Study : Geology Advisor's Signature.....

Academic Year : 2019

ACKNOWLEDGEMENTS

This senior project could not be accomplished without assistance of my advisor, Associate Professor Dr. Santi Pailoplee, who encouraged me to be creative since the first day of the project initiation and support it all the way through. My gratitude is extended to all staff of the Department of Geology, Faculty of Science, Chulalongkorn University who have been dedicated to educating me and my classmate throughout my four-year experience as an undergraduate student.

A big thank you to all my beloved GEO'60 friends for being supportive during this tough time writing our senior projects, especially during this unexpected circumstance of COVID-19 pandemic, forcing us to stay apart. Nonsense chitchat in our Line group always cheer me up.

Lastly, I would like to thank my family for being my safe zone, always support and give me advices for whatsoever the choices I made in my life.

Thampaphon Sunpa-udom

May 2020

LIST OF CONTENTS

LIST OF TABLES

LIST OF FIGURES

CHAPTER 1
INTRODUCTION

1.1. Background

Fractal is a mathematical concept of self-similarity within the geometry of shapes and often be found in nature (Mandelbrot, 1983). The concept has been used to analyze patterns found in various field of science based on different methods of calculation. Faults geometry and pattern can also be numerically determined by means of fractal dimension which is associated with the tectonic activity of the area as discussed by Hirata (1989) to classify fault types and determine the seismicity of each fault zone in Japan, Sengupta et al. (2011) to analyze distribution of seismicity in India and Sarp (2014) to characterize the neotectonics activity of each fault zone in the pull-apart basin of the East Anatolian Fault System. The most commonly used method to derive fractal dimension out of the fault geometry is the box-counting method providing characteristics of the fracture pattern (Gillespie et al., 1993). All the studies mentioned above indicate positive relationship between the fractal dimension derived from fault geometry and seismicity of the area, in other words, higher the fractal dimension of the fault geometry, higher the activity.

The mainland Southeast Asia (MLSEA) is one of the most active regions in term of tectonic activity as it is located near the plate boundary, including the Sumatra-Andaman subduction zone responsible for the M_w 9.0 earthquake in 2004. Seismic hazard evaluation of the area has been accomplished in many ways including using of active fault data (Pailoplee et al., 2009) and frequency-magnitude distribution derived from earthquake occurrences data recorded as earthquake catalogues (Pailoplee et al., 2010). Characteristics of seismic activity and distribution of seismic source in the area has also been analyzed with correlation dimension which is a perspective of fractal (Pailoplee and Choowong, 2014). However, fractal analyses focusing on fault geometry in the region are not being established well.

1.2. Objectives

1) To visualize the variation of the fractal dimension of the fault geometry in the MLSEA region.
2) To determine the relationship between the fractal dimension of the fault geometry in the MLSEA region and its seismicity parameters; e.g. b-value, a/b ratio.

1.3. Study Area

The study area is the MLSEA, covering the area between the latitude interval of 0°N to 30°N and longitude interval of 90°E to 110°E (Figure 1.1).

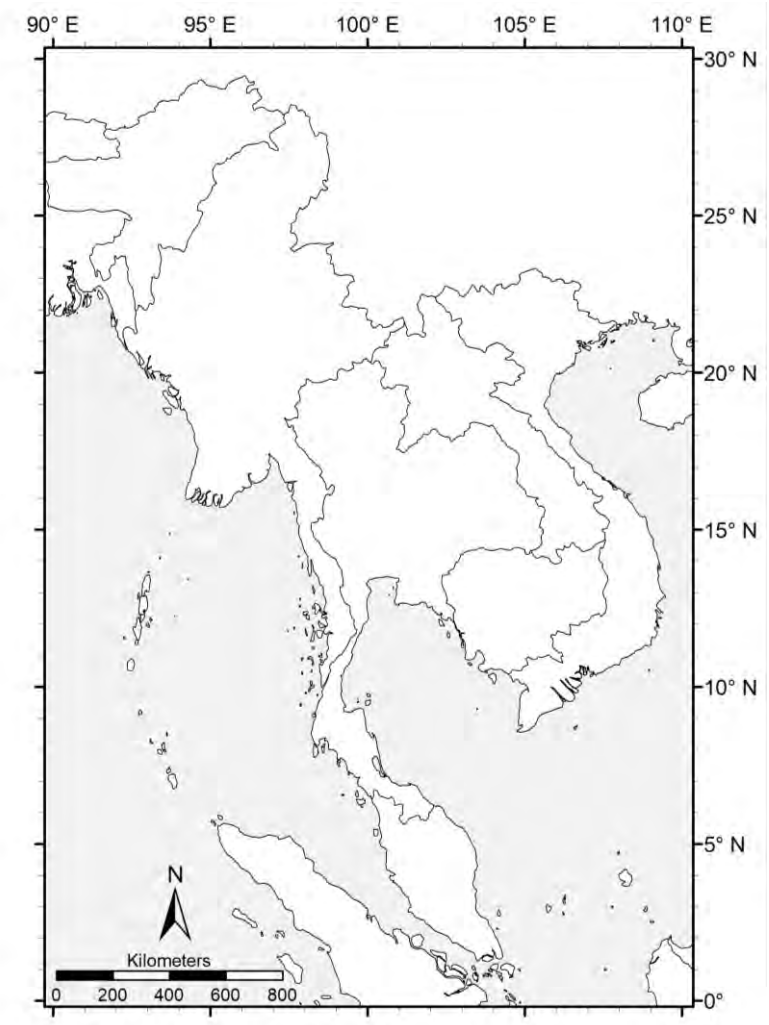

Figure 1.1 Study area map covering the MLSEA.

1.4. Scope of the Study

Focus of this study is to investigate characteristics and distribution of the fractal dimension derived from active fault geometry within the study area. Fault lines data used in this study were compiled by Pailoplee et al. (2009) and will be calculated by box-counting method using MATLAB. Finally, the fractal dimension will be correlated with the common seismicity parameters.

1.5. Expected Outcomes

1) The better understanding of the variation and distribution of the fractal dimension derived from the fault geometry in the MLSEA region.
2) Possible relationships between the fractal dimension of the fault geometry in the MLSEA region and its seismicity parameters; e.g. b-value, a/b ratio.

CHAPTER 2
THEORY AND METHODOLOGY

2.1. Regional Context

2.1.1. Tectonic setting

Regionally, the highly active seismicity of the MLSEA is a result of the Indian-Eurasian Collision started during the Middle Eocene with the convergence rate of 65 to 75 mm/year (McCaffrey, 1996). The event has caused the Sumatra-Andaman Subduction Zone along the west coast of the region and the extrusion tectonic of the Southeast Asia terrane (Tapponnier et al., 1982). Consequently, Tertiary basins of Thailand started to form in the nearly N-S trend as pull-apart basins and strike-slip fault systems started to develop or reactivate throughout the region as a result from simple shear tectonics (Poolachan and Satayarak, 1989).

The major strike-slip fault systems developed or reactivated due to the collisions includes the following—N-S trending Sagaing Fault in central Myanmar, NW-SE trending Red River Fault across China and Vietnam, western Thailand (Mae Ping, Three Pagoda, and Sri Sawat Faults), Semangko Fault along Sumatra Island, and NE-SW trending fault systems in northern Thailand (e.g. Mae Tha, Li, Long, Thoen and Phrae Faults) and southern Thailand (Ranong and Klong Marui Faults). These strike-slip fault systems and the Sumatra-Andaman Subduction Zone are responsible for seismic events throughout the region including disastrous tsunami-causing Mw 9.0 earthquake in 2004. The seismic activity of the area recorded and compiled as earthquake catalog can be visualized as shown in Figure 2.1.

The active seismicity of the area leads to studies of seismic hazard analysis to understand the behavior of earthquake events in the region and to raise precaution against possible earthquake.

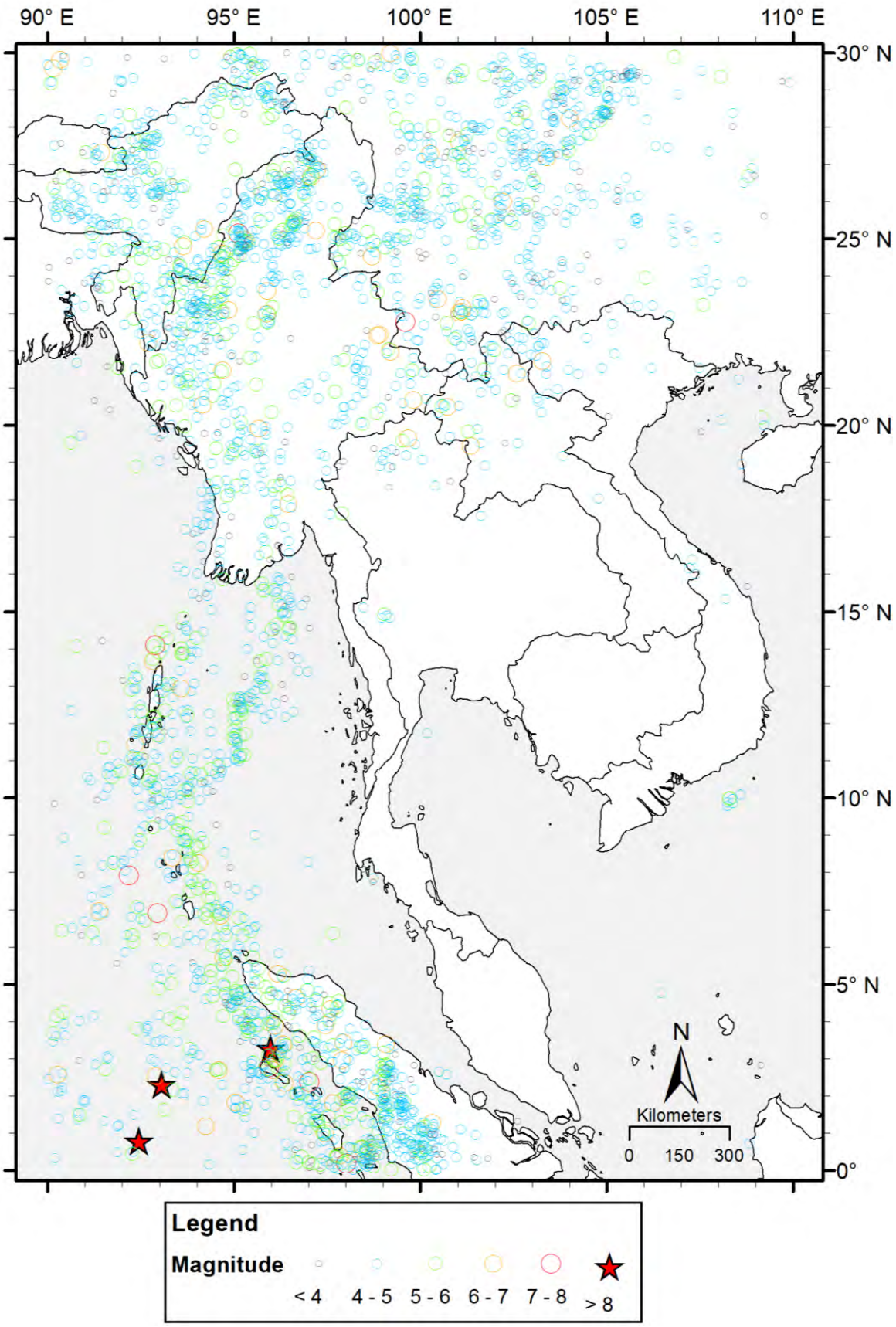

Figure 2.1 Earthquake occurrences record in the MLSEA between 1 January 1900 and 29 February 2020, retrieved from USGS earthquake database.

2.1.2. Seismotectonic provinces

To better understand and able to analyze earthquake hazard in the region more accurately, there were many attempts to divide area of the MLSEA into provinces based on its seismicity characteristics.

Nutalaya et al. (1985) pioneered the study on seismotectonic provinces of the MLSEA region and introduced 12 seismic source zones based on geological, geophysical, and seismological characteristics. However, earthquakes occurred in the area were irrelevant to those zones. Moreover, the study did not cover the area of southern peninsular Thailand and Sumatra region. Consequently, several researchers had revised the zones by combining initial evidences with modern and updated data such as epicenter of earthquakes, active faults, tectonic environments, plate boundaries, and regional geomorphology. The model of 21 seismotectonic provinces of the area was proposed by Charusiri et al. (2005) according to the disastrous earthquake and tsunami in 2004. Finally, the most recent model revised by Pailoplee and Choowong (2013) suggests the total of 13 main seismic source zones (Figure 2.2), i.e. zone A: Sumatra-Andaman Interplate, zone B: Sumatra-Andaman Intraslab, zone C: Sagaing Fault Zone, zone D: Andaman Basin, zone E: Sumatra Fault Zone, zone F: Hsenwi-Nanting Fault Zone, zone G: Western Thailand, zone H: Southern Thailand, zone I: Jinghong-Mengxing Fault Zones, zone J: Northern Thailand-Dein Bein Fhu, zone K: Song Da-Song Ma Fault Zones, zone L: Xianshuihe Fault Zone, and Zone M: Red River Fault Zone.

Recent probabilistic seismic hazard analysis of the MLSEA according to the updated 13 seismic source zones model reveal that zone A, B, and E are the most prone to earthquake occurrence with the largest annual earthquake magnitudes possible at 6.4, 5.9 and 5.7, respectively (Pailoplee and Choowong, 2013). In Thailand, however, the most active area is in the western part as a result of nearby fault zones with a 2 and 10 % POE in the next 50 years of a 0.1–0.4 g and 0.1–0.2 g PGA, respectively (Pailoplee and Charusiri, 2016).

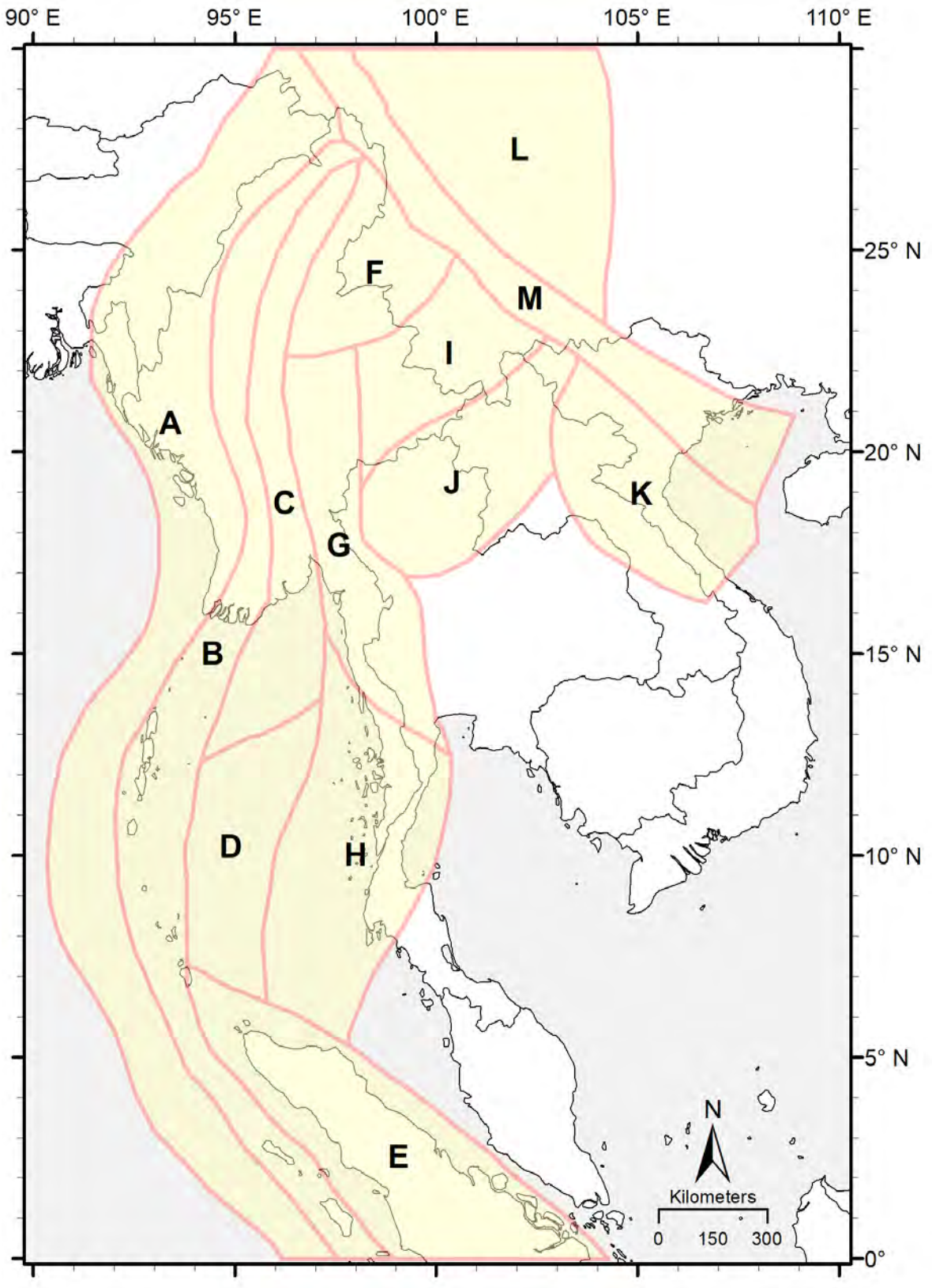

Figure 2.2 The model of 13 seismic source zones of the MLSEA, modified from Pailoplee and Choowong (2013).

2.2. Fractal Analysis

2.2.1. Fractal

Fractal is a mathematical concept of self-similarity within the geometry of shapes and often be found in nature (Mandelbrot, 1983). In the field of mathematics itself, fractal properties can be found in set of algebra and geometry, but the concept has also been used to analyze patterns found in other field of science as well. Some of the famous shapes possessing the fractal properties are Mandelbrot set—a set of complex numbers displayed on a complex plane that is valid for a specific condition of the function $f_c(z) = z^2 + c$, Sierpinski Triangle—a fractal shape with the overall shape of an equilateral triangle iteratively subdivided equally into four smaller triangle, and Koch Snowflake—a fractal shape resemble a snowflake created from iteration of same modification on each side of an equilateral triangle (Figure 2.3).

Besides the mathematical aspect, fractal pattern is also present in many objects such as branching of lightning bolt—often called Lichtenberg figure, repeating spiral of a Romanesco broccoli, and patterns of crystals (Figure 2.4). These common patterns in nature lead to studies in various fields of science to evaluate whether their complexity could be correlated to other parameters.

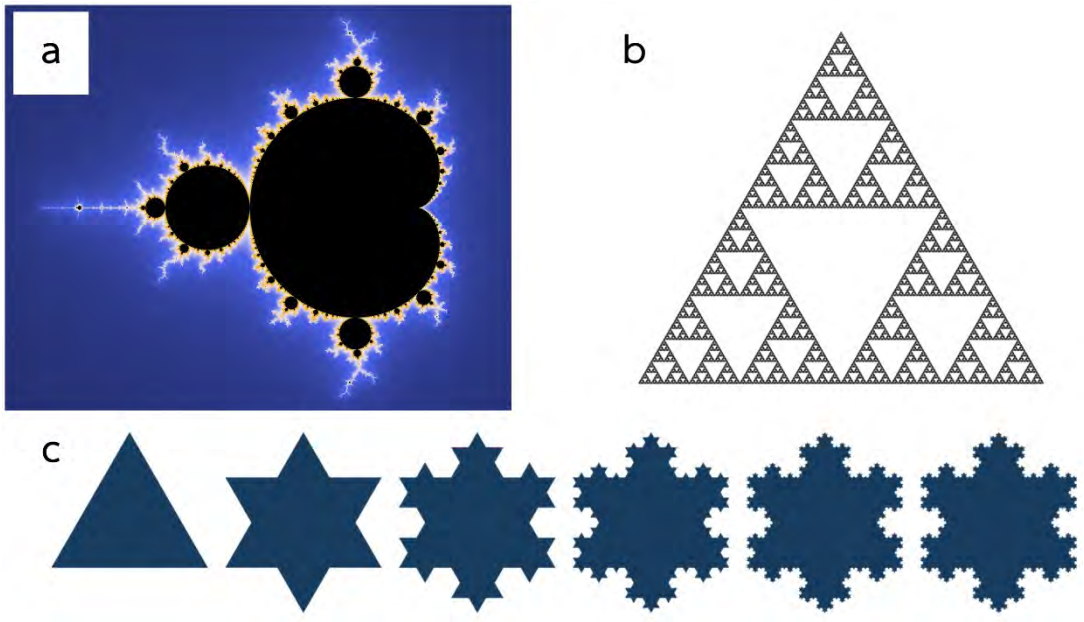

Figure 2.3 Examples of fractal objects in mathematics. a) Mandelbrot Set b) Sierpinski Triangle c) Koch Snowflake

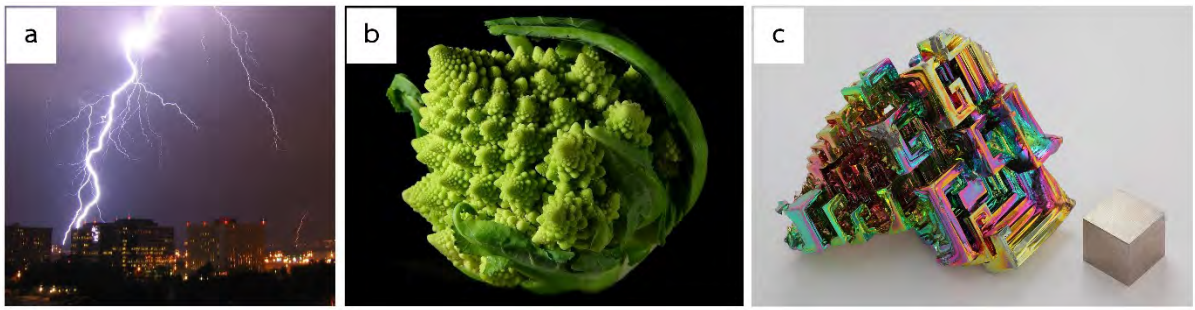

Figure 2.4 Examples of fractal patterns found in nature. a) Lichtenburg figures of lightning branches. b) Repeating spiral of Romanesco broccoli. c) Stairstep crystal structure of synthetic bismuth.

2.2.2. Fractal dimension

For a fractal pattern, its complexity could be described as fractal dimension, also called Hausdorff dimension as it was first mentioned by Felix Hausdorff in 1918. As fractal is a geometric shape of which the details do not change even observed from various scales, fractal dimension is simply a ratio of the change in detail to the change in scale (Mandelbrot, 1983).

Classical mechanics of physics and mathematics describes dimension of simple geometric shapes and forms as a whole number—dimension of a single point is zero, dimension of a segment of straight line is 1, dimension of a rectangular plane is 2, and dimension of a cube is 3. However, fractal dimension allows the measurement of complicated fractal objects as non-integer values representing the complexity in comparison to regular simple shapes. For instance, Sierpinski Triangle is a fractal shape on 2-dimensional plane composed of segments of 1-dimensional lines, thus, the fractal dimension of this figure is between 1 and 2, $\log_2 3 \approx 1.585$, to be exact.

A simple way to calculate and visualize, either the fractal dimension of a fractal object or a simple dimension of simple shapes, is to rescale the shape into a smaller piece. Number of pieces required to rebuild the original shape is the key of this visualization. Figure 2.5a adapted from Lesmoir-Gordon et al. (2000) illustrated the method of rescaling simple shapes and the calculation of its dimension. Similarly, dimension of a fractal shape can be determined by the same process as illustrated in Figure 2.5b.

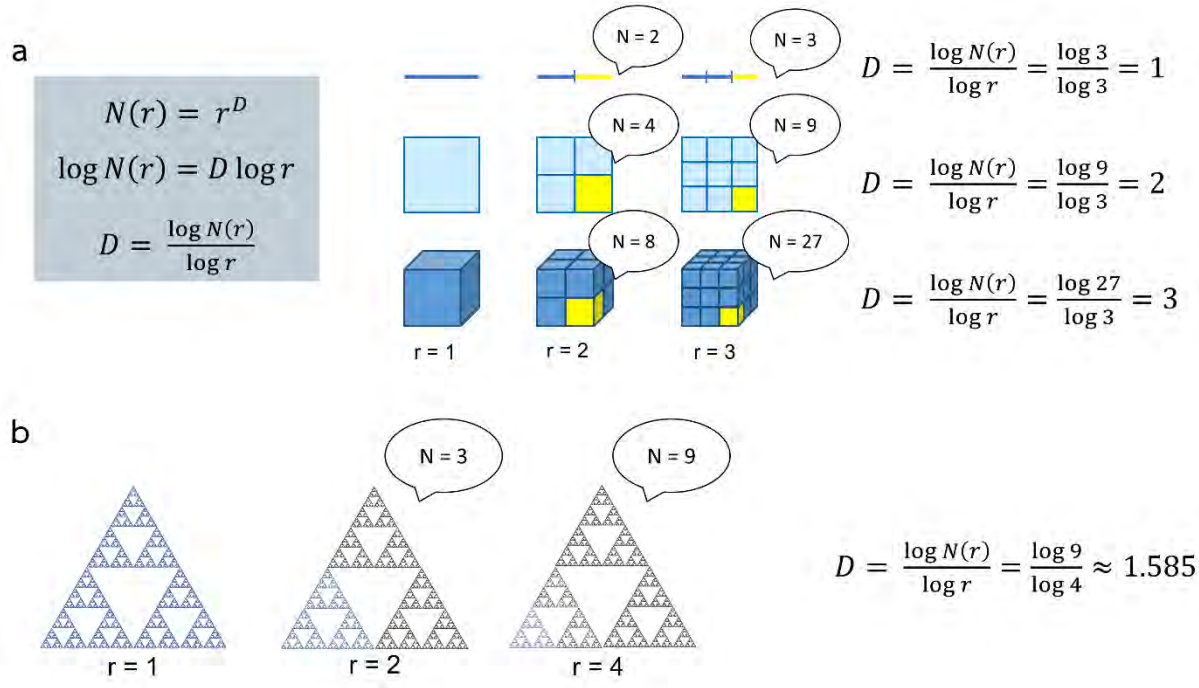

Figure 2.5 Visualization of a conventional method to calculate fractal dimension (modified from Lesmoir-Gordon et al., 2000) a) Calculation of fractal dimension of simple geometric shapes resulting in whole-number dimension. b) Calculation of fractal dimension of the Sierpinski Triangle based on the same method resulting in non-whole-number dimension.

2.2.3. Box-counting method

Conventional method to calculate fractal dimension is suitable for only geometrical fractal object as they could be easily split into components or rescaled into smaller copy of the whole. Applying such method to derive fractal dimension out of fractal irregularity in nature is a difficulty. To overcome the complication, the box-counting method, also called the Minkowski–Bouligand dimension, is used instead of the conventional method (Schroeder, 1991). The principle of the method is to rescale, instead of the object, the observation boxes and count the number of boxes that contain part of the object. The process is iterated then the total number of boxes on each side of the whole observation frame and the number of boxes containing part of the fractal object will be plot on a logarithmic scale. The slope of the plot is the fractal dimension of that object. The box-counting method is widely used in many fields of science to derive fractal dimension from irregular patterns in nature. Figure 2.6 shows the visualization of the process on an example of fault lines image.

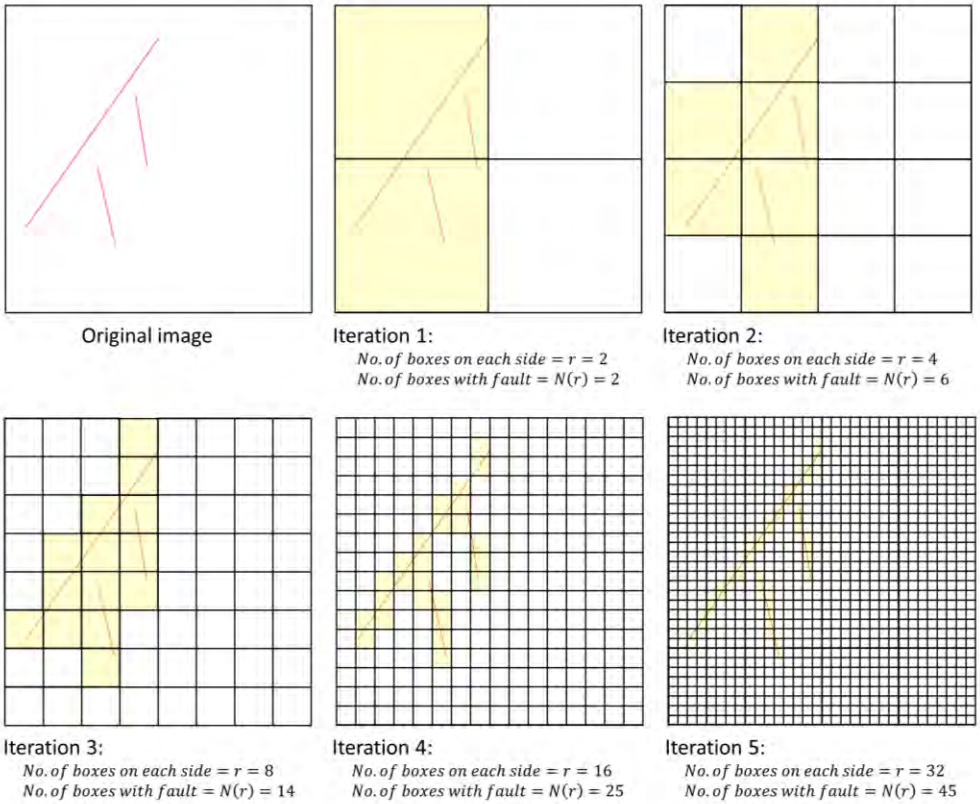

Figure 2.6 Diagram visualizing the first five iterations of box-counting algorithm.

2.3. Previous Works

Several researchers used fractal dimension derived from fault geometry as the main parameter to describe tectonic activity of their study area and correlated them with other seismicity parameters. However, there is no study focusing on the MLSEA area yet.

Sarp (2014) used fractal analysis and geomorphometric indices to study the active neotectonics of the Bingöl basin in the East Anatolian Fault System in Turkey. Fractal dimension of the study area, varies between 0.90 and 1.23, is related to the geometrical irregularity of fault lines and the tectonic influences.

Sengupta et al. (2011) studied the variation and distribution of seismicity in India based on fractal dimension of active fault lines data. The results showed positive correlation between fractal dimension and seismic activity of each region in India. The northwestern Himalayan province and the northeastern part of the country are the regions with high value

of fractal dimension that can be correlate with major earthquakes events such as 1803 Kumaon M_W 7.7, 1916 Dharchula M_W 7.1, and 1999 Chamoli M_W 6.5.

Hirata (1989) classified fault lines in Japan into 2 types which are Type I, large main fault with smaller branching, and Type II, scatter of segments without main fault. Fault lines in the center of the Japan Arc were mostly classified as Type I while those in other part were classified as Type II. Each of which was used to calculate the fractal dimension independently. The results showed that fractal dimension of the central area of the Japan Arc is relatively high, range between 1.5 to 1.6, and decreases with distance from the center. This was explained as the outer region were occupied mostly by Type II faults which are less branched.

Besides fractal analysis of fault geometry, other perspectives of fractal have been used to correlate with the seismicity as well. Pailoplee and Choowong (2014) used fractal concept to describe spatial distribution of earthquake occurrence, called the correlation dimension D_C, as a parameter to compare with b-value and a/b ratio of each seismic source zone in the MLSEA. The relationships are $D_C = 2.80 - 1.22b$ with $R^2 = 0.65$ for b-value and $D_C = 0.27\left(\frac{a}{b}\right) - 0.01$ with $R^2 = 0.68$ for a/b ratio.

2.4. Methodology

2.4.1. Literature review

Review previous studies related to proposed objectives including regional tectonic activity and seismicity of the study area, seismicity characteristics analyses based on other method that were done in the study area, and fractal analyses based on box-counting method that were done in other areas. Reviews of algorithms and software to be used for calculating the fractal dimension are also required.

2.4.2. Fault lines data gathering and processing

Active faults data compiled by Pailoplee et al. (2009) will be used in this study and have to be processed into binary raster image of appropriate resolution in order to proceed fractal analyses. Boundaries of the seismic source zones in the study area as suggested by Pailoplee and Choowong (2013) is also required.

2.4.3. Fractal analyses of faults

Fractal dimension of active fault data is to be derived in 2 perspectives.

1) Equally divided grid

Processed raster image of fault line is to be divided into equal-size grid in ArcMap then the fractal dimension value of each grid is to be calculated by box-counting method using algorithm in MATLAB.

2) According to 13 seismic source zones proposed by Pailoplee and Choowong (2013)

Processed raster image of fault line is to be clipped respect to the zoning and enclosed by square frame in ArcMap then the fractal dimension value of each zone is to be calculated by box-counting method using algorithm in MATLAB.

2.4.4. Earthquake data gathering and processing

Earthquake record of the events happened in the study area compiled by USGS is used to calculate seismicity parameters in Zmap. For comparing to fractal dimension, those seismicity variables are calculated in the same perspectives as that of faults, i.e. equally divided grid and zoning by seismic sources.

2.4.5. Results discussion and conclusion

Fractal dimension derived from equally divided grid is to determine its distribution across the study area while that derived from each seismic source zone is to be compared with the seismicity both calculated and those discussed in previous studies. Both will be analyzed and determined whether if there are any relationship between the fractal dimension and other seismicity parameters.

CHAPTER 3
DATA PREPARATION AND ANALYSIS

3.1. Fault lines

3.1.1. Raw data

To proceed fractal analysis of fault geometry, fault lines data covering whole study area is required. There are many studies involve local fault lines as their input or controlling parameter within their study area. However, only few managed to combine them into single regional consistent data. Pailoplee et al. (2009) compiled local active faults proposed by several publishers to create unified data of active fault lines and use them as a source parameter in order to evaluate seismic hazard in the MLSEA region. Thus, the data is used in this study.

Fault lines in the mentioned study are drawn based on high-resolution remote sensing data including satellite images and digital elevation model. Name of each individual fault and its termination was determined from several publications. The total number of 55 faults is proposed—covering the area of Thailand, Myanmar, Laos, Vietnam, Malaysia, Indonesia, and Southern China (Table 3.1 and Figure 3.1).

3.1.2. Processing

The original data is available as multifeatured polyline shapefile while the format required by the fractal analysis program is jpeg image, thus, processes of conversion and modification are necessary. The processes are mainly conducted in ArcGIS. Details of each step is as following (Figure 3.2).

1) Create dividing grid

To analyze the variation and distribution of fractal dimension of the study area, equally divided grid is required. In this study, three different sizes of gridding were created—1°×1°, 0.5°×0.5°, and 0.25°×0.25°.

Fault No.	*Fault zone*	*Active fault data*					*Seismicity investigation*	
		Fault type	SRL (km)	S (mm/yr)	m_{max}	A_f (km^2)	a value	b value
1	Cao Bang-Tien Yen	S	287	—	7.9	5,000	1.5	0.34
2	Chiang Rai	S	28	—	6.8	499	2.25	0.42
3	Chong Shan shear zone	S	298	5	8	6,166	7.85	1.34
4	Dein Bein Fu	S	130	2	7.5	2,163	2.68	0.37
5	Dong Trieu	S, N	187	—	7.7	3,289	2.71	0.9
6	Gaoligong Shan shear zone	S	407	5	8.1	7,603	9.67	1.62
7	Hsenwi-Nanting	S	359	1	8	6,166	25.8	4.83
8	Jinghong	S	53	—	7.1	935	2.33	0.4
9	Kawthuang	—	36	—	6.9	615	1.68	0.25
10	Klong Marui	S	29	0.1	6.8	499	1.68	0.25
11	Kungyaungale	S	25	4	6.7	405	1.68	0.25
12	Lampang-Thoen	S, N	28	0.83	6.8	499	2.72	0.55
13	Lashio	S	50	1	7	759	3.15	0.4
14	Libir	—	170	—	7.7	3,289	3.44	0.6
15	Linchang	S	107	—	7.4	1,754	2.33	0.29
16	Loei-Petchabun Suture	S	59	—	7.1	935	3.01	0.62
17	Longling-Ruili	S	70	5	7.2	1,153	6.42	1.01
18	Mae Chaem	—	21	—	6.6	328	1.89	0.32
19	Mae Chan	S	99	3	7.4	1754	2.64	0.37
20	Mae Hong Sorn-Tak	S	37	—	6.9	615	2.65	0.38
21	Mae Ing	S	38	—	6.9	615	2.56	0.38
22	Mae Tha	S	47	0.8	7	759	2.36	0.38
23	Mae Yom	S	22	0.8	6.6	328	1.92	0.6
24	Menglian	S	117	0.5	7.5	2,163	2.13	0.28
25	Mengxing	S	75	4.8	7.3	1,422	2.95	0.4
26	Moei-Tongyi	S	259	0.73	7.9	5,000	3.46	0.54
27	Nam Ma	S	177	2.4	7.7	3,289	3.18	0.58
28	Nam Peng	S	51	—	7.1	935	3.08	0.59
29	Ongkalak	S, N	47	0.17	7	759	2.52	0.4
30	Pa Pun	S	143	—	7.6	2,667	2.58	0.37
31	Pan Luang	S	219	—	7.8	4,055	2.98	0.51
32	Pha Yao	S, N	20	0.1	6.6	328	2.95	0.4
33	Phrae	S	28	0.1	6.8	499	2.68	0.53
34	Pua	N	29	0.6	6.8	499	2.44	0.55
35	Qiaohou	—	145	—	7.6	2,667	2.35	0.25
36	Ranong	S	46	1	7	759	1.68	0.25
37	Red River	S	812	4	8.5	17,579	17.6	3.16
38	Sagiang-Sumatra	S	958	23	8.5	17,579	6.92	0.86
39	Shan	S	66	—	7.2	1,153	2.93	0.39
40	Song Ca	S	225	—	7.8	4,055	2.58	0.48
41	Song Chay	S, N	55	2	7.1	935	3.05	0.58
42	Song Da	S	46	—	7	759	2.73	0.45
43	Song Ma	S	72	—	7.2	1,153	6.52	1.06
44	Sri Sawat	S	43	2	7	759	2.5	0.4
45	Andaman subduction	R	3,388	47	9.2	76,208	6.08	0.69
46	Tavoy	S	32	—	6.8	499	2.8	0.79
47	Tenasserim	S	50	4	7	759	1.68	0.25
48	Tha Khaek	S	250	—	7.9	5,000	3.15	0.67
49	Three Pagoda	S	141	2	7.6	2,667	2.62	0.51
50	Uttaladith	S	27	0.1	6.7	405	1.63	0.46
51	Wan Na-awn	—	69	—	7.2	1,153	2.28	0.35
52	Wanding	S	199	1.9	7.7	3,289	5.34	0.93
53	Wang Nua	—	31	—	6.8	499	2.27	0.4
54	Xianshuihe	S	505	15	8.2	9,376	6.74	1.05
55	Hutgyi	S, R	5	0.03	5.9	76	1.67	0.34

Table 3.1 Summary of seismic parameters of the 55 active fault zones in the MLSEA (modified from Pailoplee et al., 2009). SRL is surface rupture length (km), m_{max} is maximum possible earthquake magnitude, A_f is rupture area (km^2), and S is slip rate (mm/yr). Fault type: S = strike-slip fault, N = normal fault, R = reverse fault.

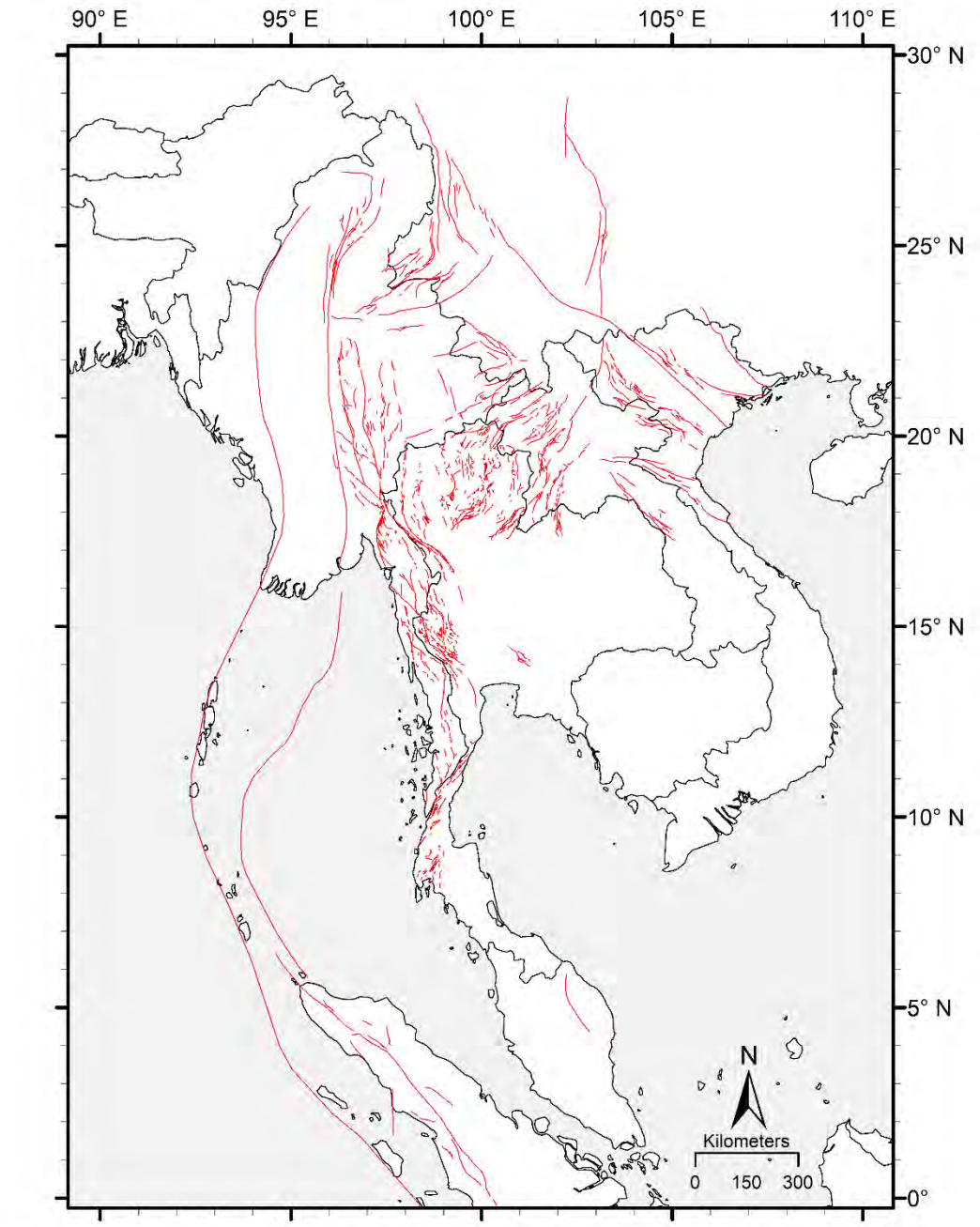

Figure 3.1 Fault lines of the MLSEA (Pailoplee et al., 2009).

2) Convert the fault lines to raster

Resolution of the output is critical for fractal analysis. The fractal dimension calculation algorithm requires resolution of the jpeg image to be 2^n by 2^n and the resolution of 1024 by 1024 pixels will be used in this study. Accordingly, cell size assigned to the converted fault lines must be equal to the grid size divided by 1024. The output file is formatted as tiff file for further modification.

3) Modify the fault lines raster

Suitable format is required in order to export raster file as jpeg—RGB, 8-bit unsigned integer formatted raster. To satisfy this requirement, the fault lines raster has to be reclassified to contain unique value for describing the existence of fault. After that, the reclassed raster must be copied to create applicable format. The raster is then exported as jpeg.

4) Split the fault lines to each grid

The final jpeg image is then be clipped according to each grid. Each of which is to be analyzed by fractal dimension calculation algorithm in MATLAB individually.

3.1.3. Fractal analysis of fault lines

After processing the raw data, the output of fault line images is ready for fractal dimension calculation algorithm. The MATLAB scripts used in this project was modified from Anoop (2011) in purpose to read multiple images and store the calculation value after execution of the program. The stored values are derived from each plot including fractal dimension (slope of plot), y-axis interception, and mean squared error of trendline fitting.

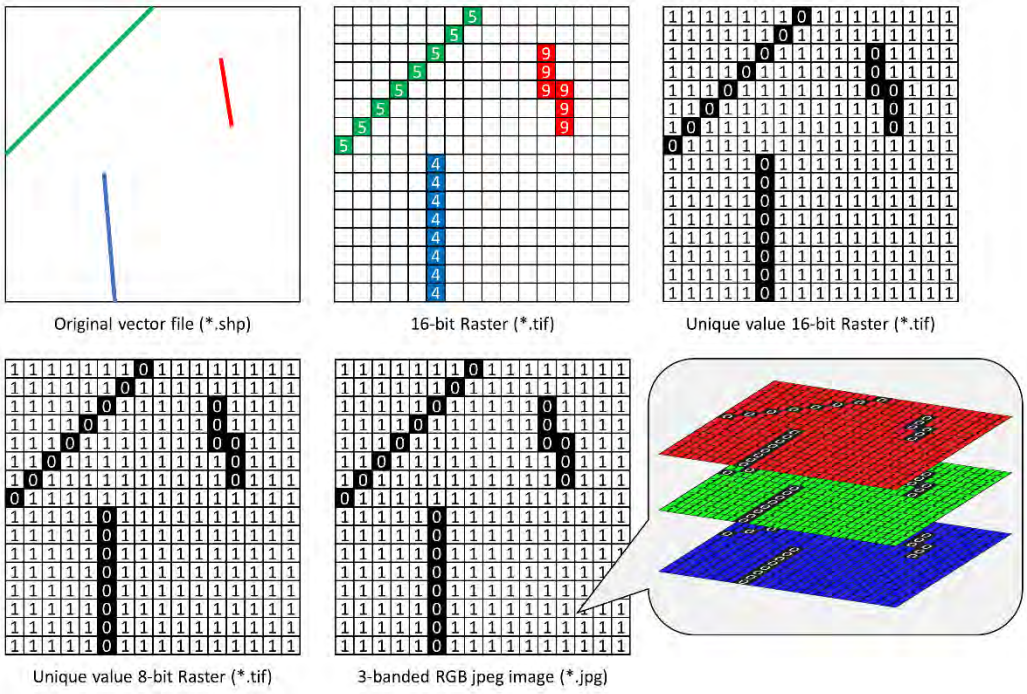

Figure 3.2 Diagram showing steps of processing fault lines data.

3.2. Earthquake catalog

3.2.1. Database

Earthquake catalog used in this study was compiled by USGS, accessible from USGS website (https://earthquake.usgs.gov/earthquakes/). The queries for list of the seismic events are those with magnitude ranging between 1 and 10 happened from 1 January 1900 to 29 February 2020 within boundary of the study area, latitude interval of 0°N to 30°N and longitude interval of 90°E to 110°E.

The original data comprises 17,893 events of earthquake with histogram for some of its statistics as shown in Figure 3.3. This raw set of data is highly distorted due to large amount of foreshock and aftershock from the M_w 9.0 earthquake in 2004.

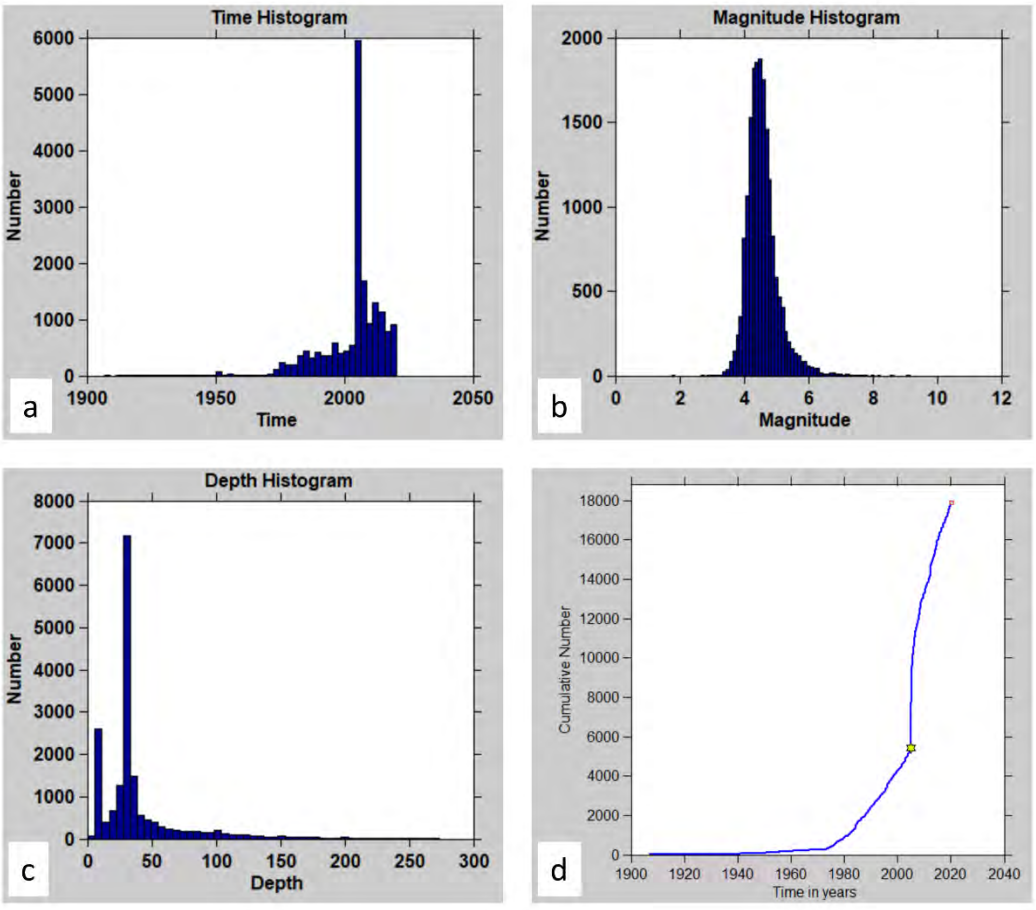

Figure 3.3 Histograms of raw earthquake data statistics. a) Time Histogram b) Magnitude Histogram c) Depth Histogram d) Cumulative Time Histogram

3.2.2. Processing

Earthquakes record obtained from USGS must be processed to filter out foreshocks and aftershocks which are not related directly to the tectonic influences. There were many algorithms that were proposed to de-cluster the seismic records and achieve suitable data, however, the model of Gardner and Knopoff (1974) is applied in this study. The process of de-clustering detects 1,241 clusters of earthquakes and eliminates 14,824 records (98.85%) which were not main shocks. Statistics of the remaining 3,069 tectonic-induced seismic activities are shown in Figure 3.4.

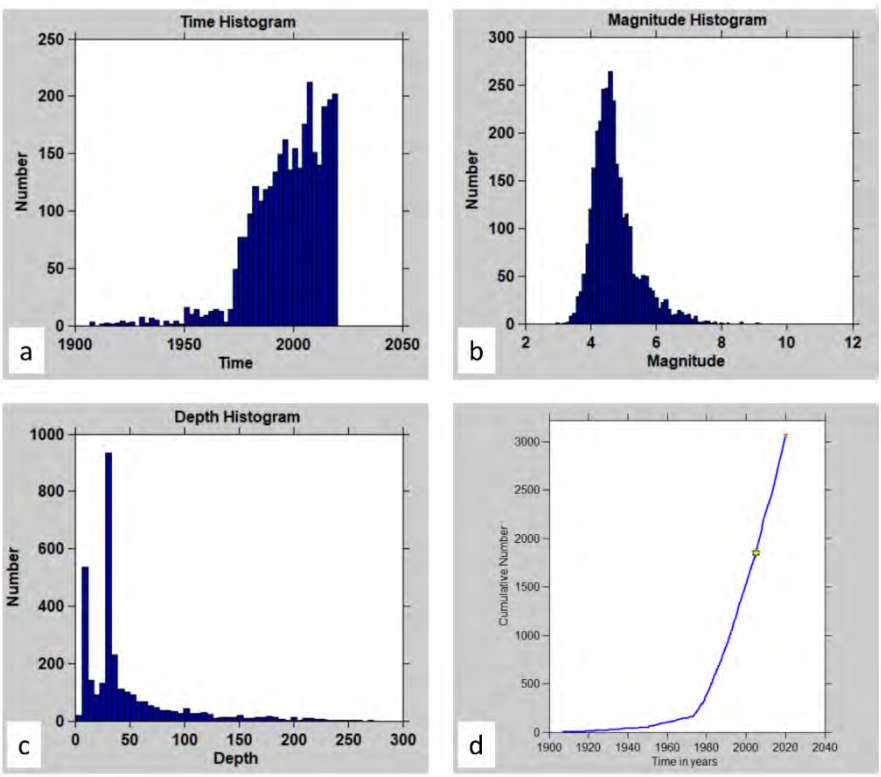

Figure 3.4 Histograms of earthquake data statistics after de-clustering (Gardner and Knopoff, 1974). a) Time Histogram b) Magnitude Histogram c) Depth Histogram d) Cumulative Time Histogram

Theoretically, cumulative number of earthquake occurrence is a linear relationship with time because the tectonic activity within the timespan of measurement is relatively constant. However, Figure 3.4d suggests two segments of linear relationship. The reason for the abrupt change of slope around year 1970 is because of overall sensitivity of seismic recording instrument. Thus, to ensure the consistency of the analysis, only earthquake data contributed in the later part of the graph will be used. Finally, the meaningful quantitative earthquake catalog derived from the MLSEA region contains 2,911 events of seismic

occurrence with some statistics shown in Figure 3.5. Some seismicity parameters are calculated including $b - value = 0.811 \pm 0.02$, $a - value = 6.89$, and magnitude of completeness $M_c = 4.5$. Frequency-magnitude distribution plot of earthquake occurrence in the study area is shown in Figure 3.5e.

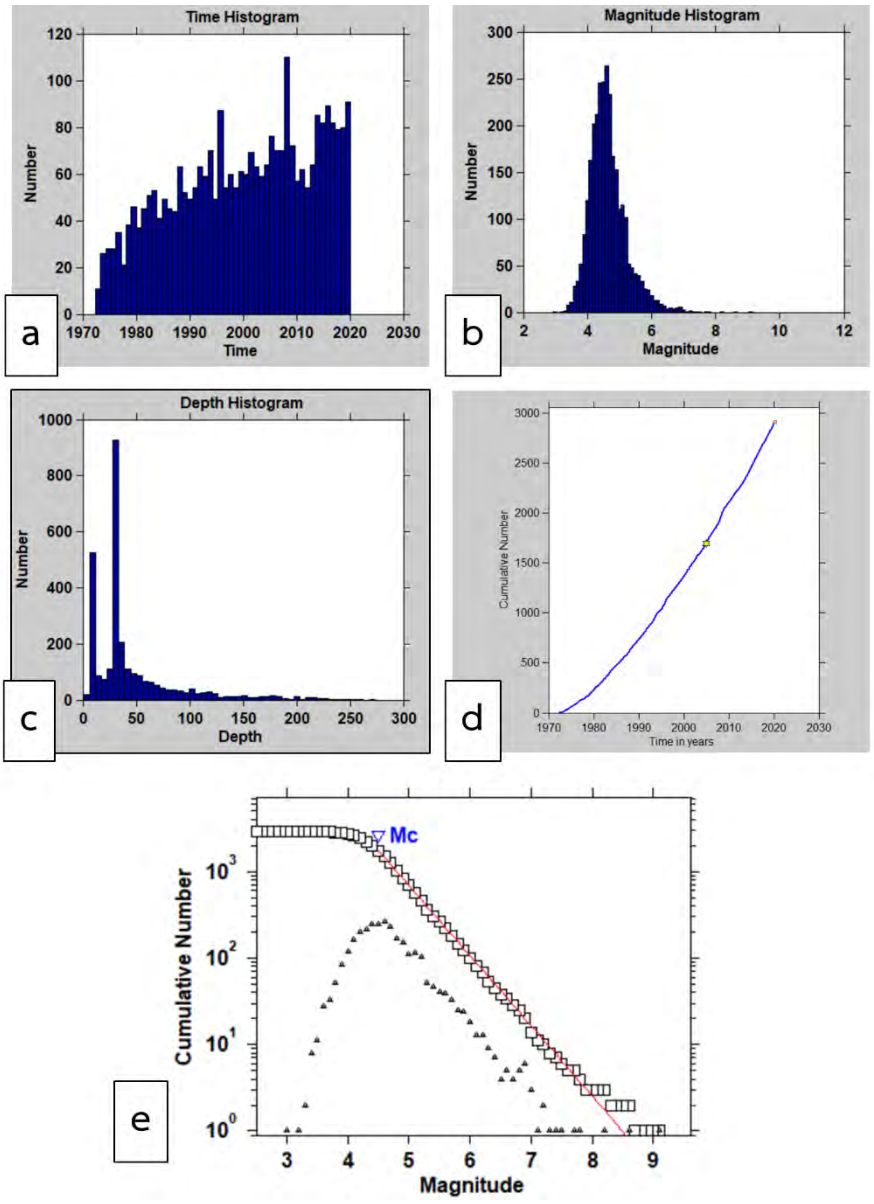

Figure 3.5 Histograms of complete earthquake data statistics. a) Time Histogram b) Magnitude Histogram c) Depth Histogram d) Cumulative Time Histogram e) Frequency-magnitude distribution plot of seismic records in the study area.

CHAPTER 4

RESULTS

This chapter focuses on variation and distribution map of fractal dimension derived from fault lines geometry that were processed as discussed in CHAPTER 3. The maps are shown in three perspectives divided as sections in this chapter. Relationship between fractal dimension and other seismicity parameters, however, will be discussed in CHAPTER 5.

4.1. Regional scale

As mentioned in CHAPTER 3, three sizes of equally divided grid are applied to cover the study area of the MLSEA, i.e. 1°×1°, 0.5°×0.5°, and 0.25°×0.25°. After selecting only grid squares that contain part of fault lines, there are 189, 503, and 1,257 grid squares for each grid size, respectively. Each of the fault image representing each grid is selected as an input for box-counting algorithm that create a plot for each image and store the calculated values for further analysis (Figure 4.1). The values are then be assigned to the grid and displayed as map (Figure 4.2–4.4). All three maps show expected characteristics that the value of fractal dimension is greater with higher complexity of fault lines within each grid. The value ranges from approximately 0.3 to 1.2 in all grid sizes. However, the fractal dimension value of less than 0.8 is considered an outlier which will be discussed in topic 5.1 in CHAPTER 5.

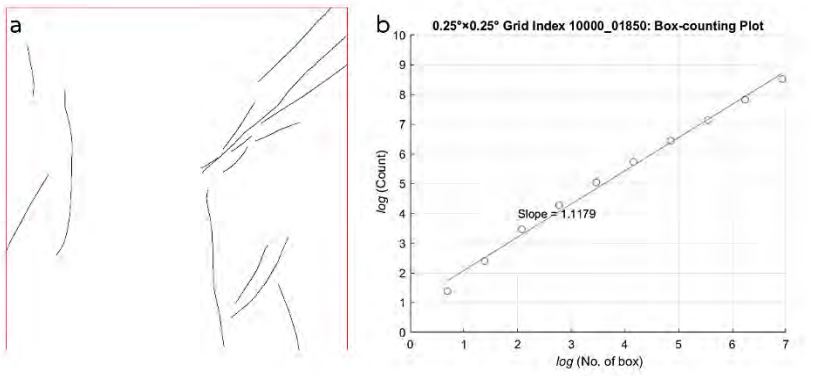

Figure 4.1 Example of fractal analysis by box-counting method. a) A fault image extracted from 0.25°×0.25° grid. b) Box-counting plot acquired from the fault image.

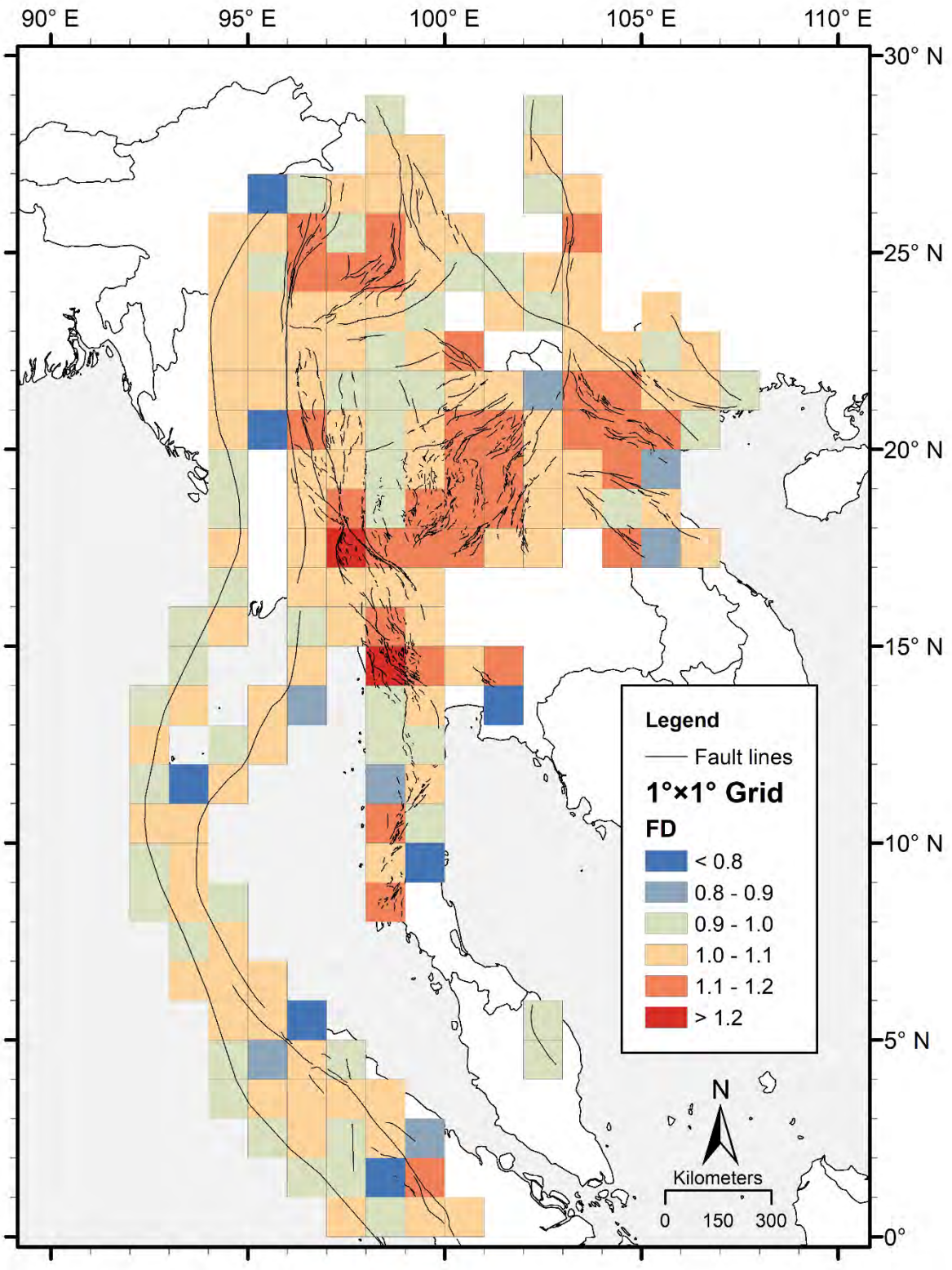

Figure 4.2 Variation and distribution map of fractal dimension in the MLSEA by the grid of 1°×1°.

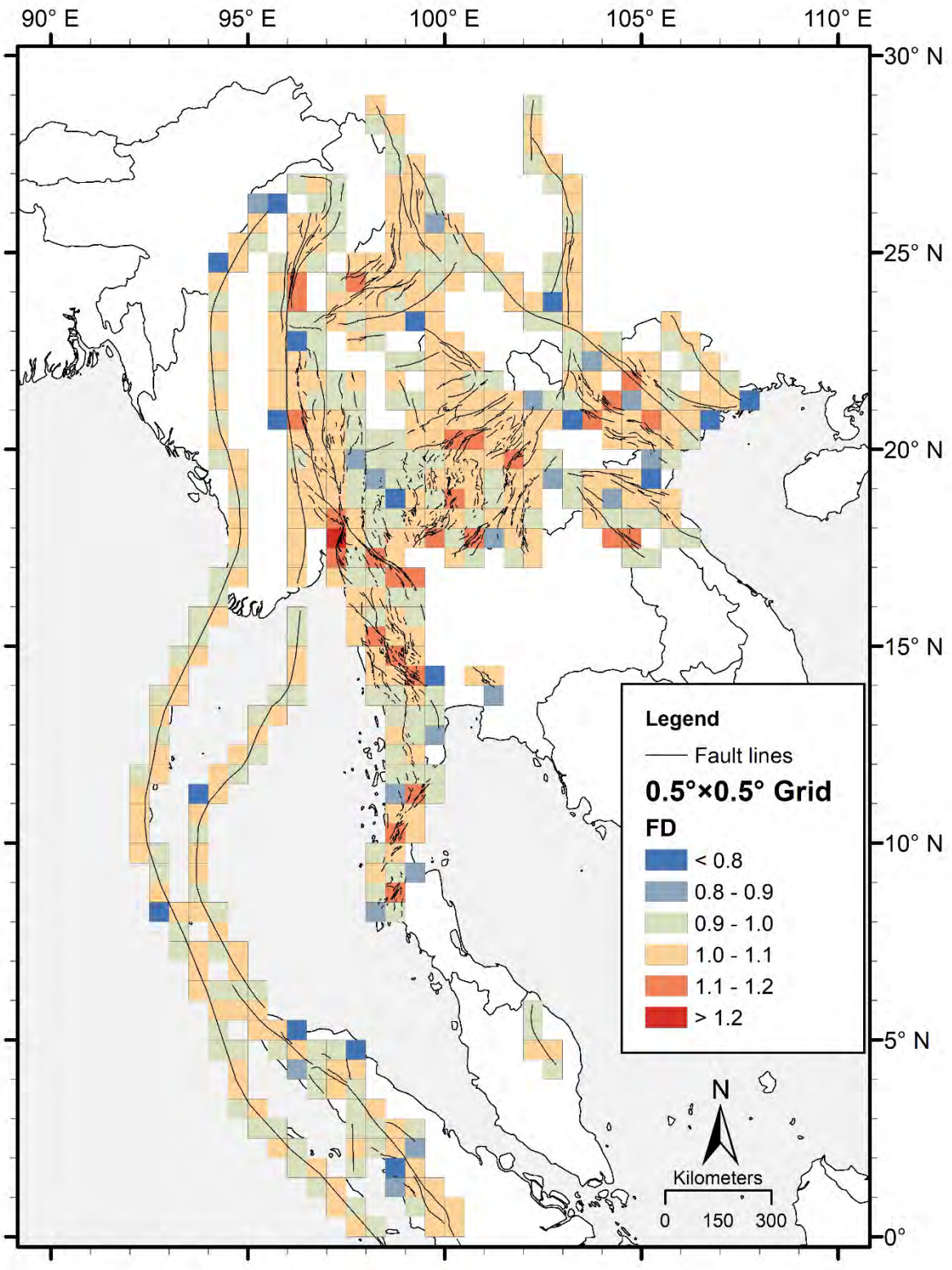

Figure 4.3 Variation and distribution map of fractal dimension in the MLSEA by the grid of 0.5°×0.5°.

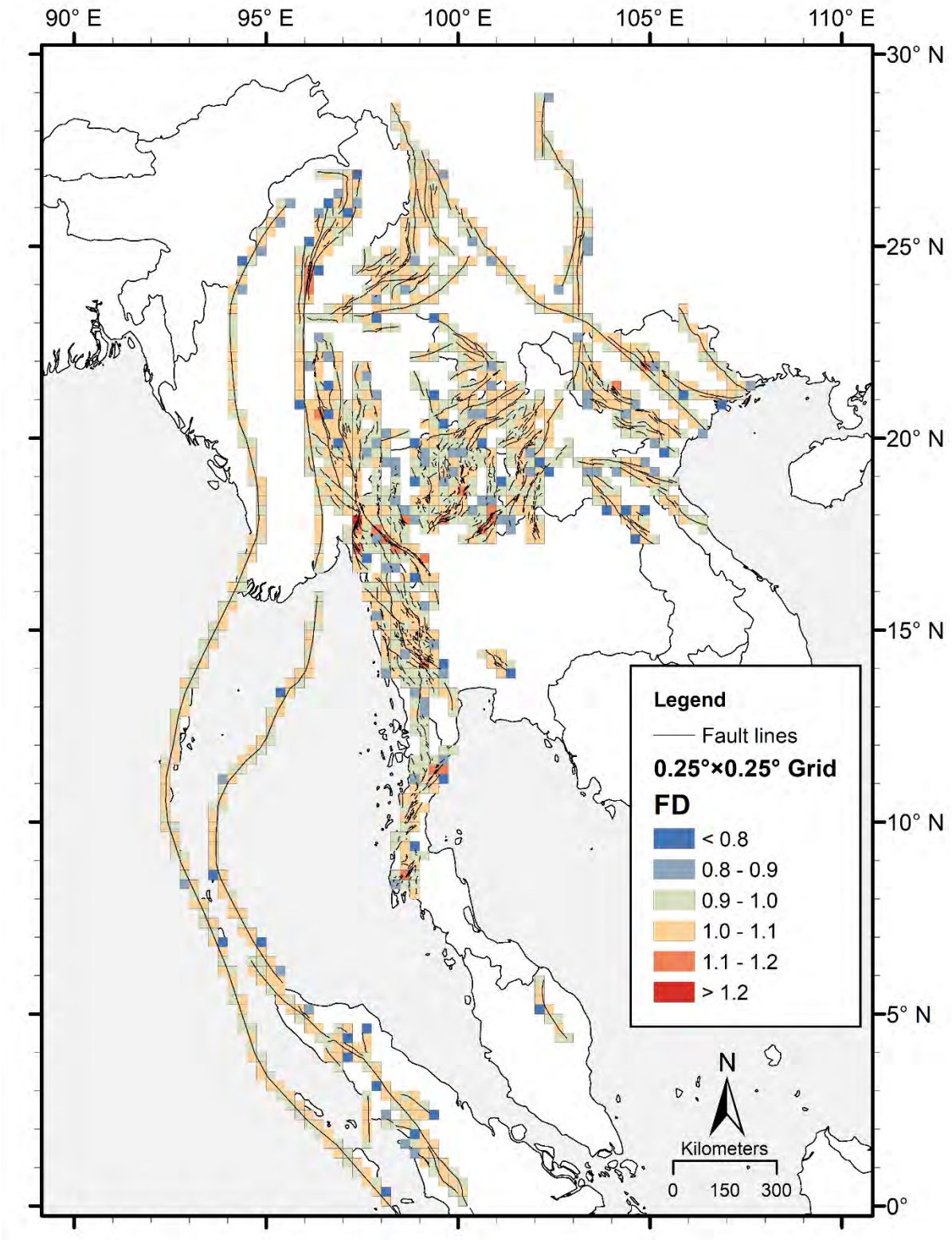

Figure 4.4 Variation and distribution map of fractal dimension in the MLSEA by the grid of 0.25°×0.25°.

4.2. Major seismic-prone zones

In this section, distribution maps of fractal dimension are displayed based on several specific areas to emphasize variation of the value in those regions. Five zones are selected as they are seismic-prone with records of many earthquake events.

4.2.1. Sumatra-Andaman Subduction Zone

According to the compilation by Pailoplee et al. (2009), fault lines in this area are mostly long, straight, and non-branched. This resulted in low to moderate value of fractal dimension, ranging from 0.292 to 1.071 for 0.5°×0.5° gridding and ranging from 0.346 to 1.065 for 0.25°×0.25° gridding. Grid squares with comparatively low value of fractal dimension are those with very small segment of fault lines passing through and could be considered as outliers (further discussion in topic 5.1 in CHAPTER 5).

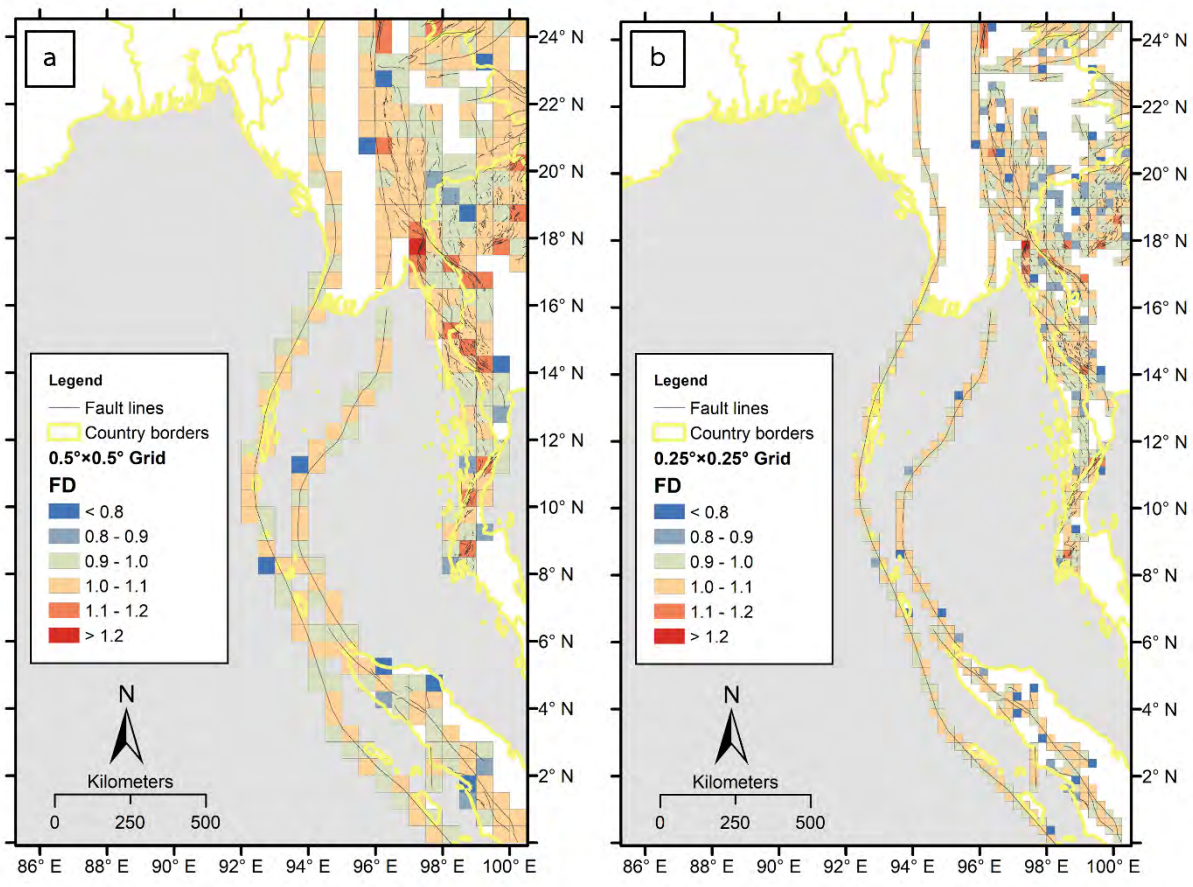

Figure 4.5 Variation and distribution map of fractal dimension in the region of Sumatra-Andaman Subduction Zone. a) by the grid of 0.5°×0.5°. b) by the grid of 0.25°×0.25°.

4.2.2. Sagaing Fault Zone

Fractal dimension along the Sagaing Fault Zone in the central Myanmar ranges from 0.758 to 1.253 for 0.5°×0.5° gridding and ranges from 0.673 to 1.229 for 0.25°×0.25° gridding. The localities with significantly high value of fractal dimension are labeled in Figure 4.6.

1) The area in the vicinity of Indaw town, Katha District, where Sagaing main fault started to branch near the termination in the north. The value of fractal dimension is 1.133–1.177 in 0.5° grid and 1.111–1.135 in 0.25° grid.
2) The middle point between Mandalay and Nay Pyi Taw. The value of fractal dimension is 1.103 in 0.5° grid and 1.117 in 0.25° grid.
3) The complex branching of Pa Pun Fault where the value of fractal dimension is 1.253 in 0.5° grid and 1.155–1.229 in 0.25° grid.

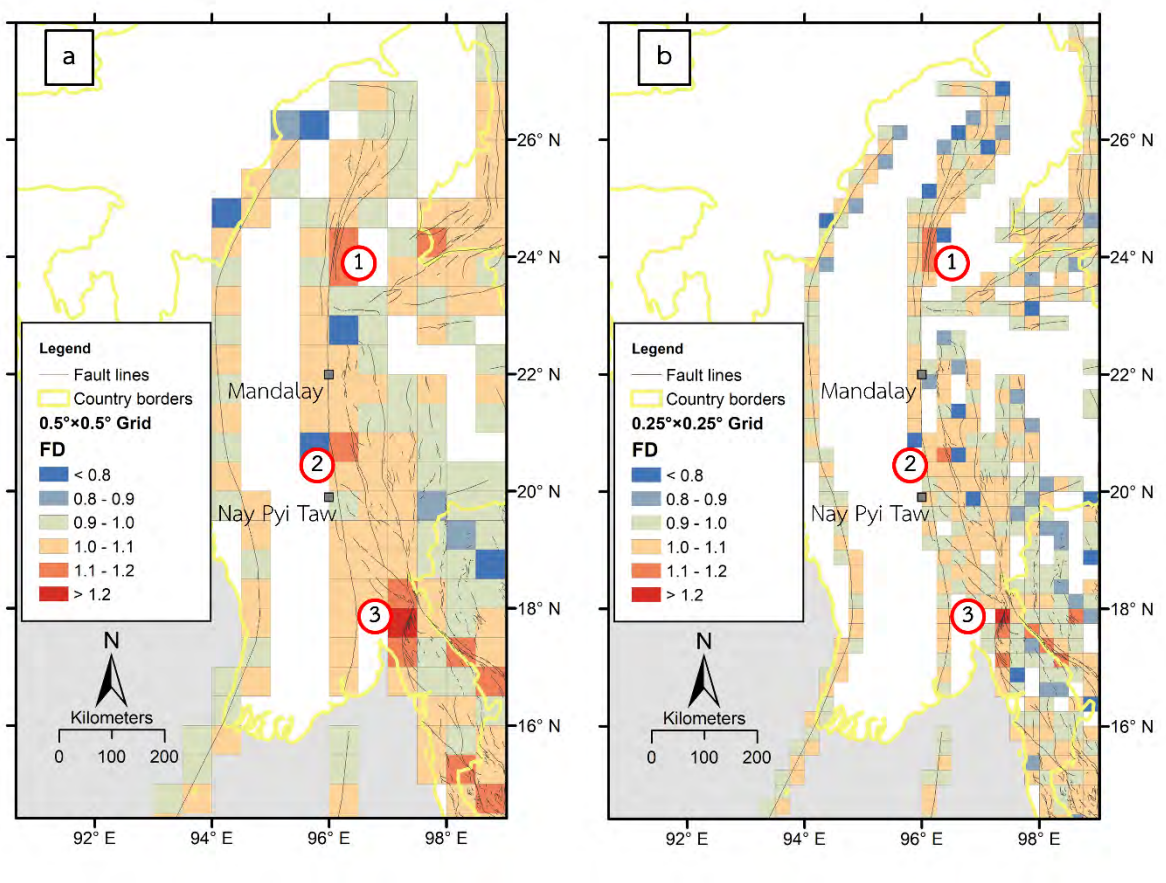

Figure 4.6 Variation and distribution map of fractal dimension in the region of Sagaing Fault Zone with labels of areas of significantly high value. a) by the grid of 0.5°×0.5°. b) by the grid of 0.25°×0.25°.

4.2.3. Northern Thailand

Characteristics of faults in Northern Thailand and around Thailand-Laos-Myanmar border is mostly short and segmented, therefore, there is a drastic effect from rescaling from 0.5° grid box to 0.25° grid box and resulted in boxes with comparatively low fractal dimension (further discussion in topic 5.2 in CHAPTER 5). The value of fractal dimension ranges from 0.654 to 1.176 for 0.5°×0.5° gridding and ranges from 0.279 to 1.135 for 0.25°×0.25° gridding. The localities with significantly high value of fractal dimension are labeled in Figure 4.7.

1) The vicinity of Mae Ing, Mae Chan, and Chiang Rai faults. The value of fractal dimension is 1.106–1.119 in 0.5° grid.
2) Segments of Dein Bein Fu fault near Luang Phrabang, Laos. The value of fractal dimension is 1.114 in 0.5° grid.
3) The vicinity of Mae Yom, Phrae, Pha Yao, and Lampang-Thoen faults. The value of fractal dimension is 1.121 in 0.5° grid and 1.063–1.118 in 0.25° grid.
4) Segments of Phrae fault. The value of fractal dimension is 1.155 in 0.5° grid and 1.114 in 0.25° grid.
5) The vicinity of Uttaladith and Dein Bein Fu faults in Uttaradit Province. The value of fractal dimension is 1.176 in 0.5° grid and 1.118–1.133 in 0.25° grid.
6) Along Moei-Tongyi and Mae Hong Sorn-Tak faults in Tak Province. The value of fractal dimension is 1.106–1.150 in 0.5° grid and 1.104–1.135 in 0.25° grid.

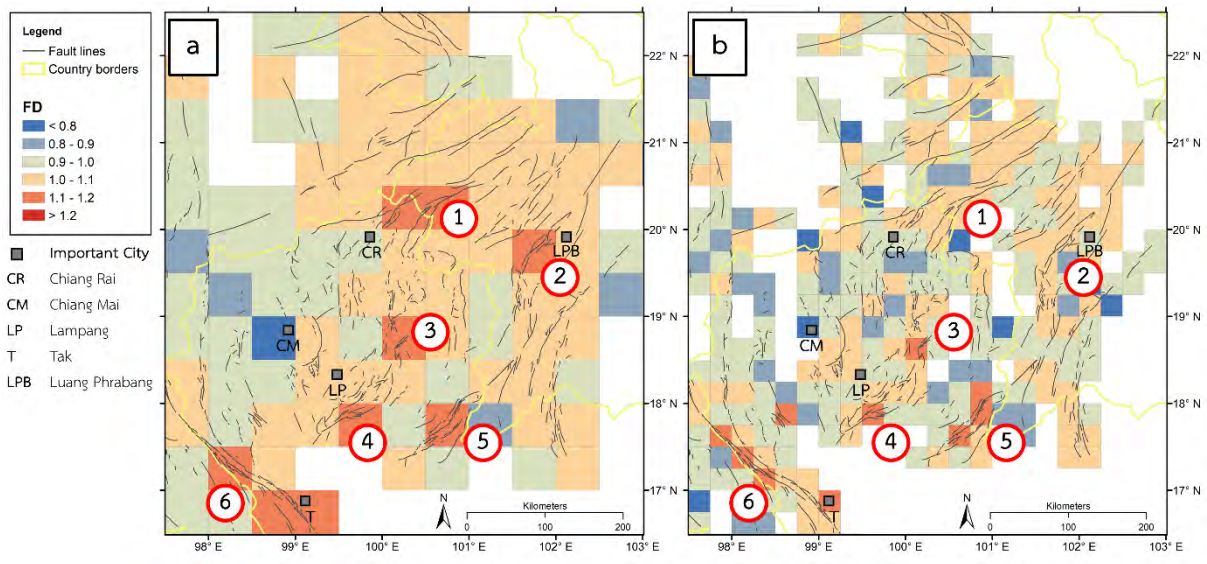

Figure 4.7 Variation and distribution map of fractal dimension in Northern Thailand with labels of areas of significantly high value. a) by the grid of 0.5°×0.5°. b) by the grid of 0.25°×0.25°.

4.2.4. Western Thailand

Similar to Northern Thailand, faults in the Western Thailand is short and segmented resulting in the same effect from rescaling. The value of fractal dimension ranges from 0.629 to 1.184 for 0.5°×0.5° gridding and ranges from 0.474 to 1.140 for 0.25°×0.25° gridding. The only area with significantly high value of fractal dimension is situated along the Thailand-Myanmar border where there are Three Pagoda, Sri Sawat, and parts of Tavoy faults. The fractal dimension is 1.116–1.184 in 0.5° grid and 1.140 in 0.25° grid.

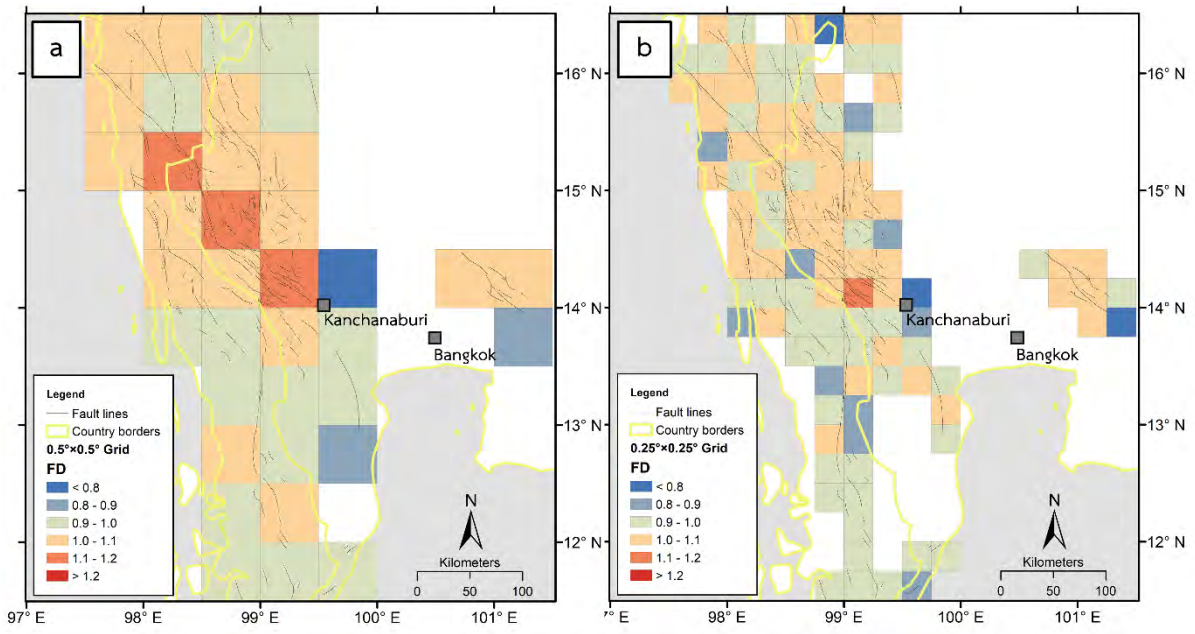

Figure 4.8 Variation and distribution map of fractal dimension in Western Thailand. a) by the grid of 0.5°×0.5°. b) by the grid of 0.25°×0.25°.

4.2.5. Southern Thailand

In Southern Thailand, the value of fractal dimension ranges from 0.868 to 1.138 for 0.5°×0.5° gridding and ranges from 0.531 to 1.148 for 0.25°×0.25° gridding. The localities with significantly high value of fractal dimension are labeled in Figure 4.9.

1) Parts of Ranong, and Kawthuang faults in lower part of Prachuap Khiri Khan Province. The value of fractal dimension is 1.109 in 0.5° grid and 1.106–1.108 in 0.25° grid.
2) Parts of Ranong fault in Ranong Province. The value of fractal dimension is 1.131 in 0.5° grid.
3) Parts of Klong Marui fault in Surat Thani Province. The value of fractal dimension is 1.138 in 0.5° grid and 1.148 in 0.25° grid.

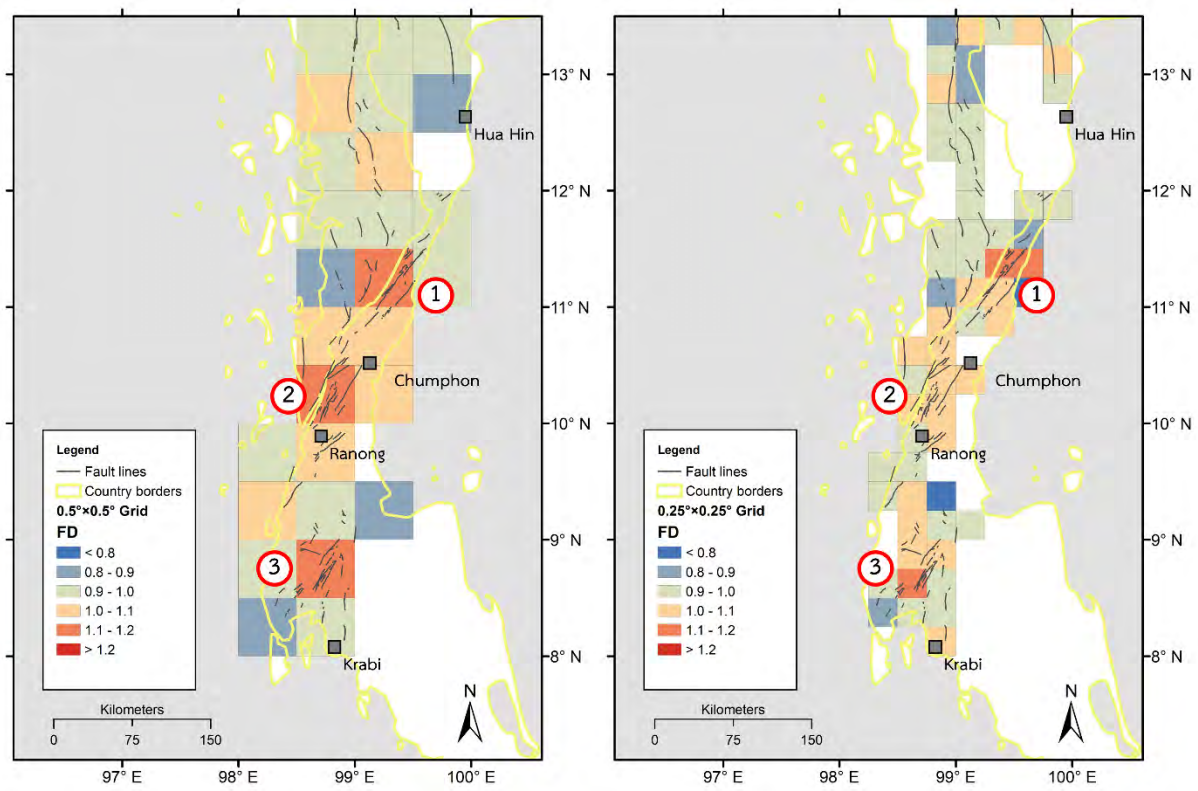

Figure 4.9 Variation and distribution map of fractal dimension in Southern Thailand with labels of areas of significantly high value. a) by the grid of 0.5°×0.5°. b) by the grid of 0.25°×0.25°.

4.3. According to 13 seismic source zones

Fault lines data is extracted according to 13 seismic source zones suggested by Pailoplee and Choowong (2013) and used as an input for fractal dimension calculation algorithm. The value of fractal dimension ranges from the lowest of 0.906 in Zone D to the highest of 1.194 in Zone G.

Besides fractal analysis, seismicity parameters are also calculated from seismic events to reflect seismic characteristics of each zone. Frequency-magnitude distribution plots of earthquake occurrence in each seismic source zone are shown in Figure 4.10. Seismicity parameters and fractal dimension derived from fractal analysis are summarized in Table 4.1. Finally, the variation and distribution map of fractal dimension of the MLSEA by seismic source zones is shown in Figure 4.11. Noted that the scale for fractal dimension value is slightly different from previous maps.

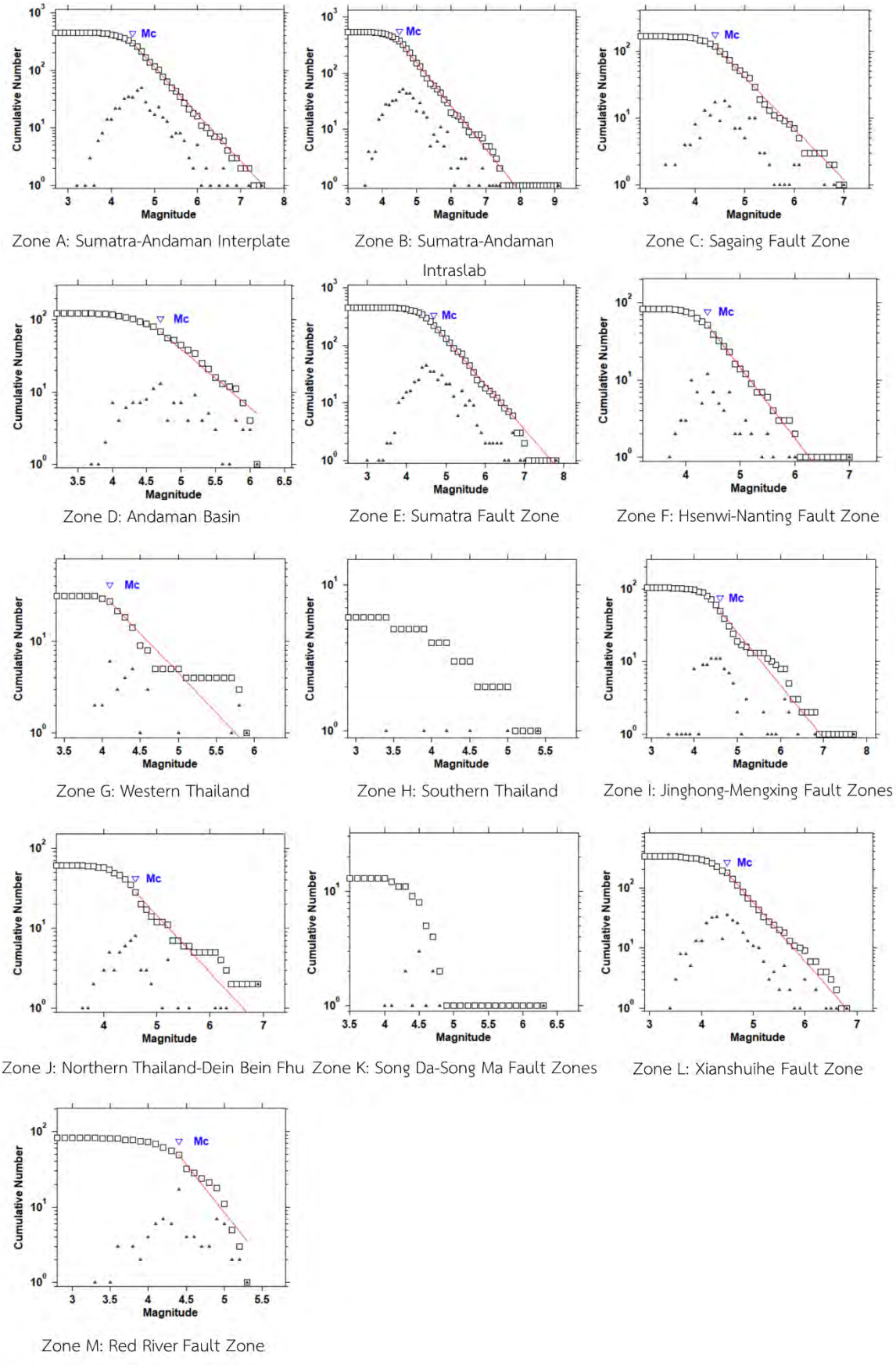

Figure 4.10 Frequency-magnitude distribution plots of seismic activity in each seismic source zone in the MLSEA.

Seismic source zones	*Seismicity parameters*				*Fractal dimension*
	EQ Number	M_C	a-value	b-value	
A: Sumatra-Andaman Interplate	454	4.5	6.15	0.818	0.94634
B: Sumatra-Andaman Intraslab	536	4.5	6.03	0.768	0.97801
C: Sagaing Fault Zone	166	4.4	5.44	0.767	1.0212
D: Andaman Basin	123	4.7	5.65	0.811	0.90578
E: Sumatra Fault Zone	452	4.7	6.04	0.787	1.0292
F: Hsenwi-Nanting Fault Zones	82	4.4	5.73	0.913	1.0602
G: Western Thailand	31	4.1	4.98	0.865	1.1935
H: Southern Thailand	9	—	—	—	1.0952
I: Jinghong-Mengxing Fault Zones	104	4.6	5.06	0.731	0.98975
J: Northern Thailand-Dein Bein Phu	61	4.6	4.74	0.715	1.1619
K: Song Da-Song Ma Fault Zones	13	—	—	—	1.1332
L: Xianshuihe Fault Zone	332	4.5	6.66	0.98	1.0152
M: Red River Fault Zone	82	4.4	7.28	1.27	1.0271

Table 4.1 Summary of seismicity parameters calculated in Zmap and fractal dimension calculated in MATLAB based on 13 seismic source zones.

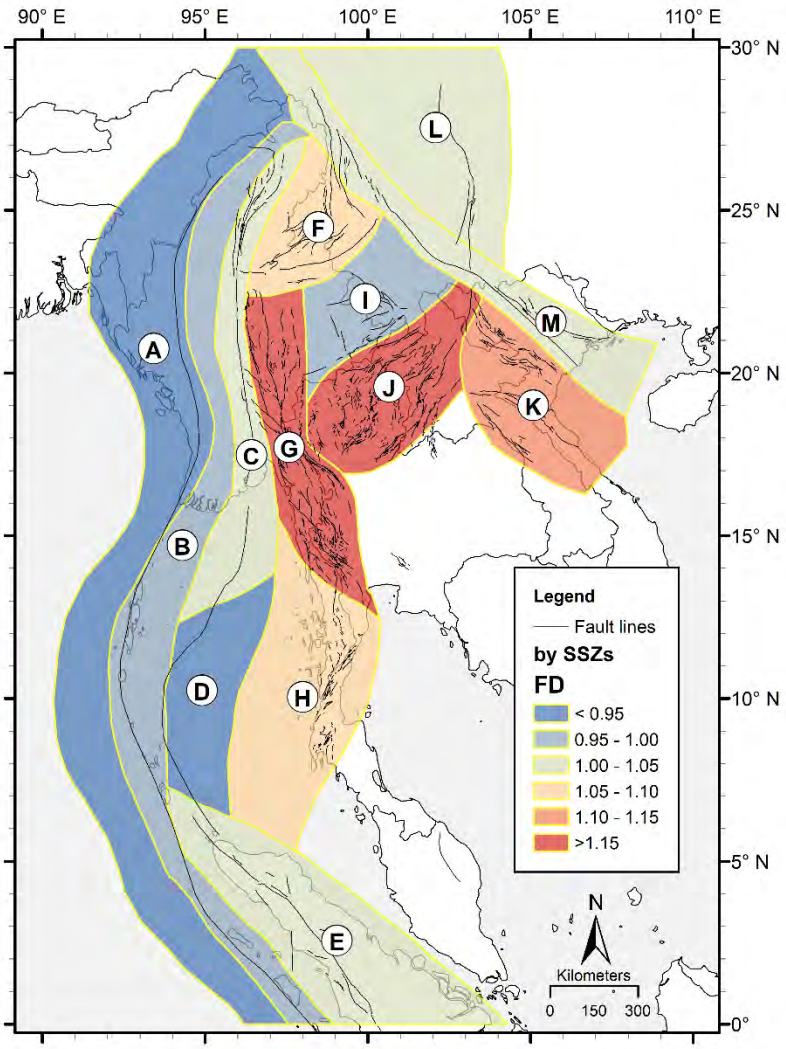

Figure 4.11 Variation and distribution map of fractal dimension in the MLSEA based on 13 seismic source zones.

CHAPTER 5
DISCUSSION AND CONCLUSION

5.1. Fractal dimension outliers

Most of the fractal dimension values derived from the box-counting method range from 0.8 to 1.2 and mean squared error of <0.1. However, there are some outliers, with the fractal dimension of <0.8 and much more statistical error. Those outliers are calculated from grids that contain little amount of black pixel representing segments of fault lines, resulting in significant error during linear fitting process in MATLAB script. Examples of box-counting plot from both the grid square that follow normal trend and that of the outliers are illustrated in Figure 5.1.

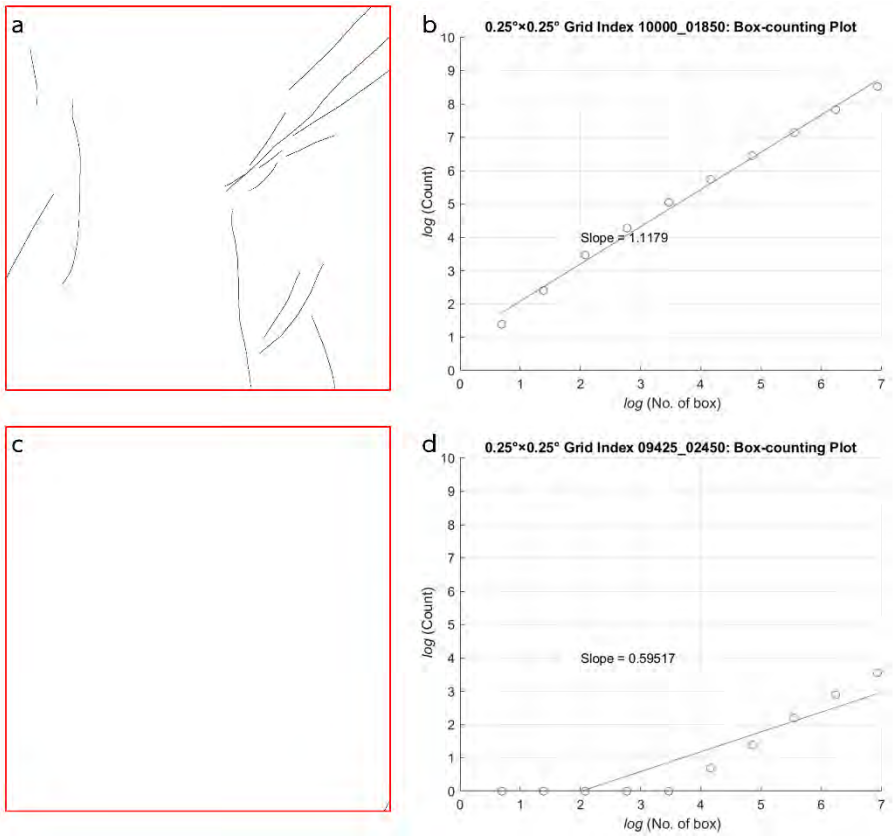

Figure 5.1 Example of outliers in the result of 0.25°×0.25° grid. a-b) A typical grid with well-distributed pixel containing fault lines resulting in normal box-counting plot with sensible trend line. c-d) A grid with too little amount of pixel containing fault lines (bottom right corner of the image) resulting in distorted, large error box-counting plot.

Distribution of mean squared error and fractal dimension value (Figure 5.2–5.5) provides the guideline for choosing grid squares with valid interval of fractal dimension. Generally, those with fractal dimension larger than 0.8 have mean squared error less than 0.1 and therefore valid for further discussion.

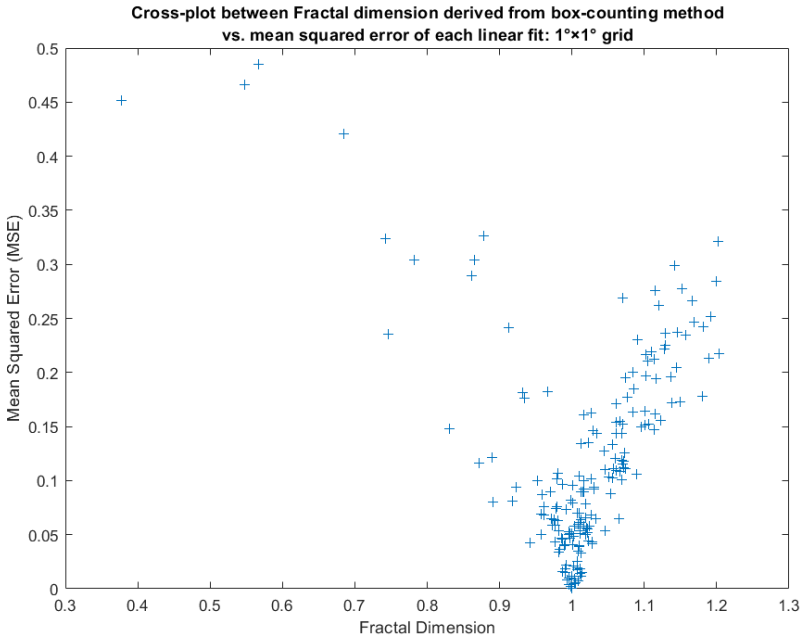

Figure 5.2 Scatter plot between fractal dimension and mean squared error of linear fit from each grid square in 1°×1° grid.

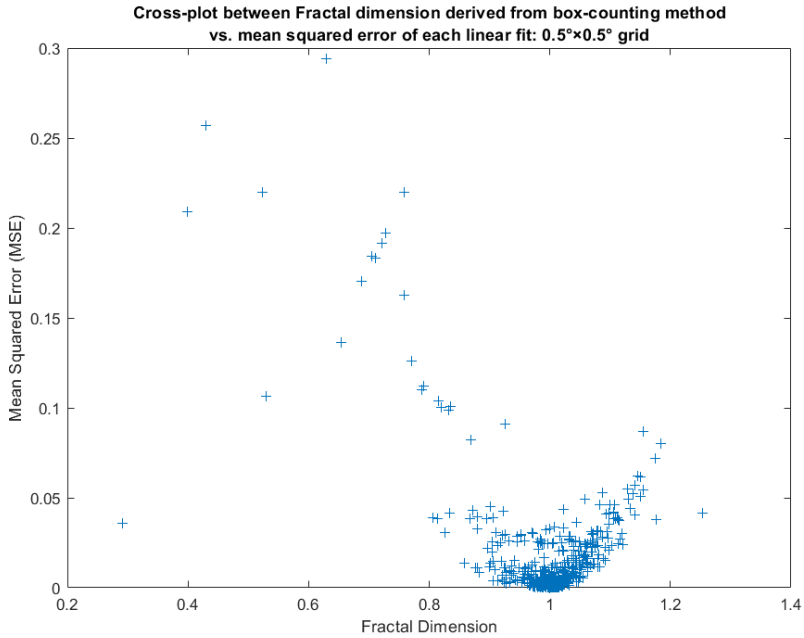

Figure 5.3 Scatter plot between fractal dimension and mean squared error of linear fit from each grid square in 0.5°×0.5° grid.

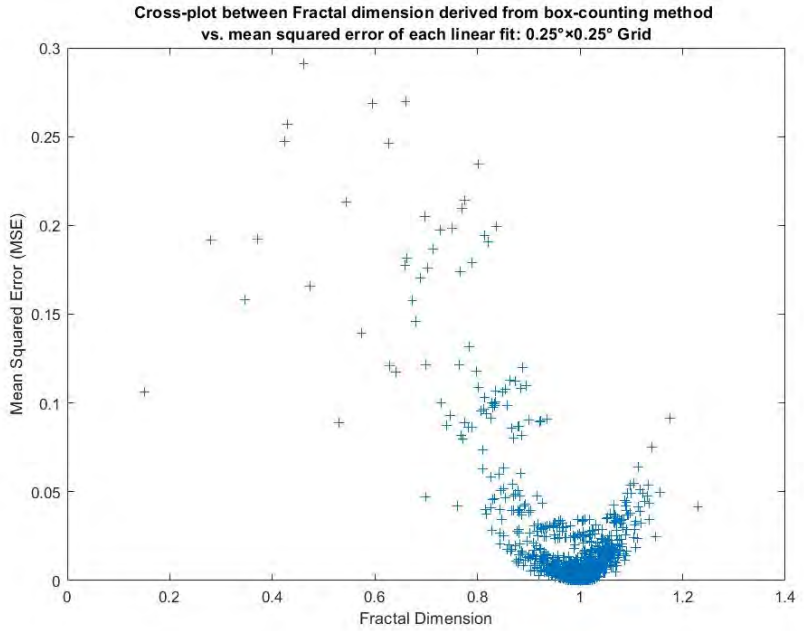

Figure 5.4 Scatter plot between fractal dimension and mean squared error of linear fit from each grid square in 0.25°×0.25° grid.

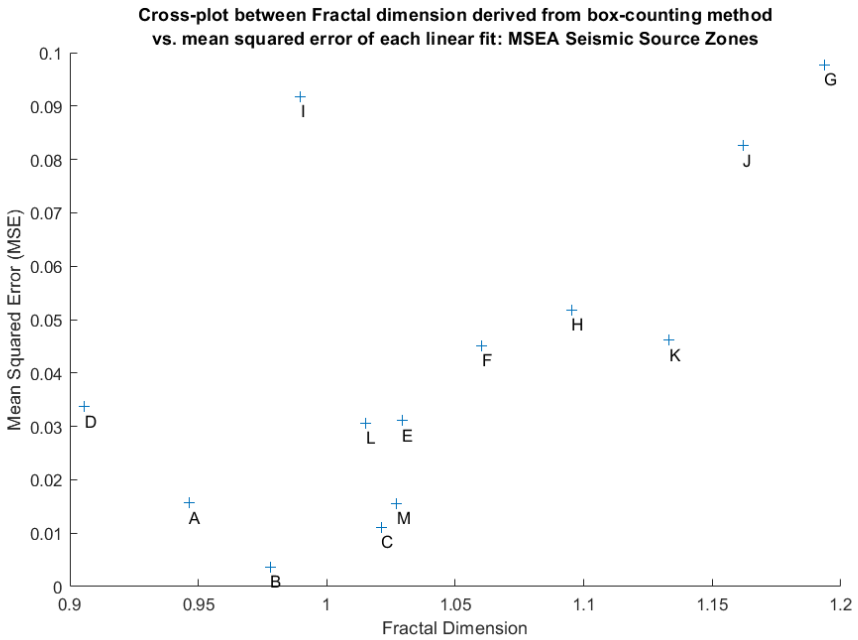

Figure 5.5 Scatter plot between fractal dimension and mean squared error of linear fit from each zone of the 13 seismic source zones.

5.2. Rescaling effects

Fractal is usually used to describe complexity independently from scale of observation. Intuitively, we might expect that the value of fractal dimension is distributed likewise—similar distribution irrelevant to the size of observation grid spacing. However, variation and distribution map of fractal dimension in some seismic-prone area shows differences in the distribution. The fault lines divided into smaller grid spacing, 0.25°×0.25°, returned higher ratio of low fractal dimension compared to those observed in larger grid size.

As fractal dimension is a measurement of complexity of fault lines in each image as a whole, dividing it further into smaller images can re-distribute those complexity and increase the ratio of low fractal dimension area. This effect is more likely to occur in the area with short and segmented faults as there is higher possibility that those fault lines will be separated when rescaled, e.g. Northern Thailand and Western Thailand. This effect of rescaling can be explained in simple visualization shown in Figure 5.6.

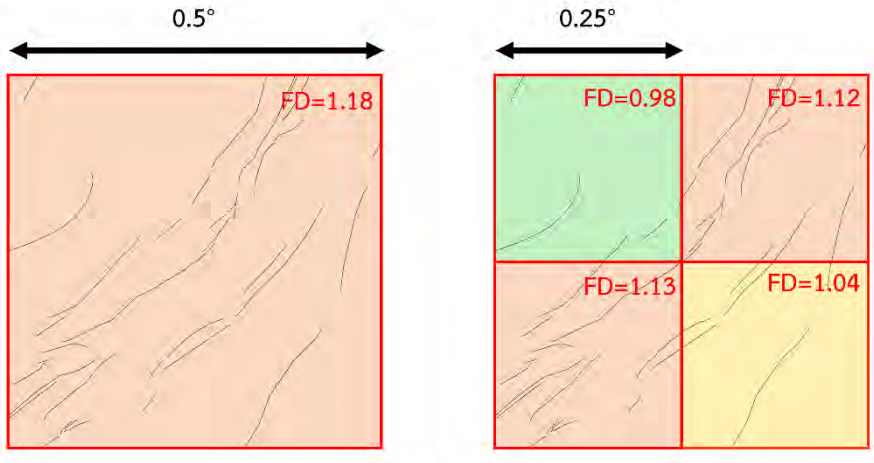

Figure 5.6 Visualization of rescaling effect. The two images of faults lines are from the same area, longitude 100.5°–101.0° and latitude 17.5°–18.0°. Further division of fault lines images also reduces complexity of the fault as whole.

5.3. Correlation by regional scale

Various seismicity parameters of the MLSEA were calculated from earthquake record as mentioned in CHAPTER 3. The calculation was based on 3 three different grid spacings in such way that is correlatable to the fractal dimension. The scatter plots of fractal dimension and seismicity parameters are displayed based on these three grid sizes. Both fractal dimension which is the slope of the box-counting plot and y-axis intercept are being plotted to emphasis any possible relationship.

Among the 189 grid squares of the 1°×1° spacing, only 151 squares can correlate to seismicity parameters. The total of 403 and 1,009 squares are suitable for 0.5°×0.5° and 0.25°×0.25° spacings, respectively. The plots shown in Figure 5.7–5.9 are scatter plots illustrating values of fractal dimension and y-axis intercept against various seismicity parameters—a-value, b-value, a/b ratio, and magnitude of completeness. However, there is no significant relationship between either fractal dimension or y-axis intercept to any of the seismicity parameters. Instead of expected linear relationships, the plots of fractal dimension show dense cluster of data around the area where fractal dimension value is equal to 1 while the plot of y-axis intercept show no significant clustering.

5.4. Correlation by seismic source zone

Seismicity parameters of the MLSEA were also calculated based on the 13 seismic source zones model and be correlatable to the fractal dimension that was derived from the same manner. Moreover, correlation dimension (D_C) of each seismic source zone calculated from previous study (Pailoplee and Choowong, 2014) is used for the comparison as well. The plots shown in Figure 5.10–5.11 are scatter plots illustrating values of fractal dimension and y-axis intercept against various seismicity parameters based on the seismic source zone. However, there are only few possible relationships present as negative linear regression trend but with very poor coefficient of determination (R^2).

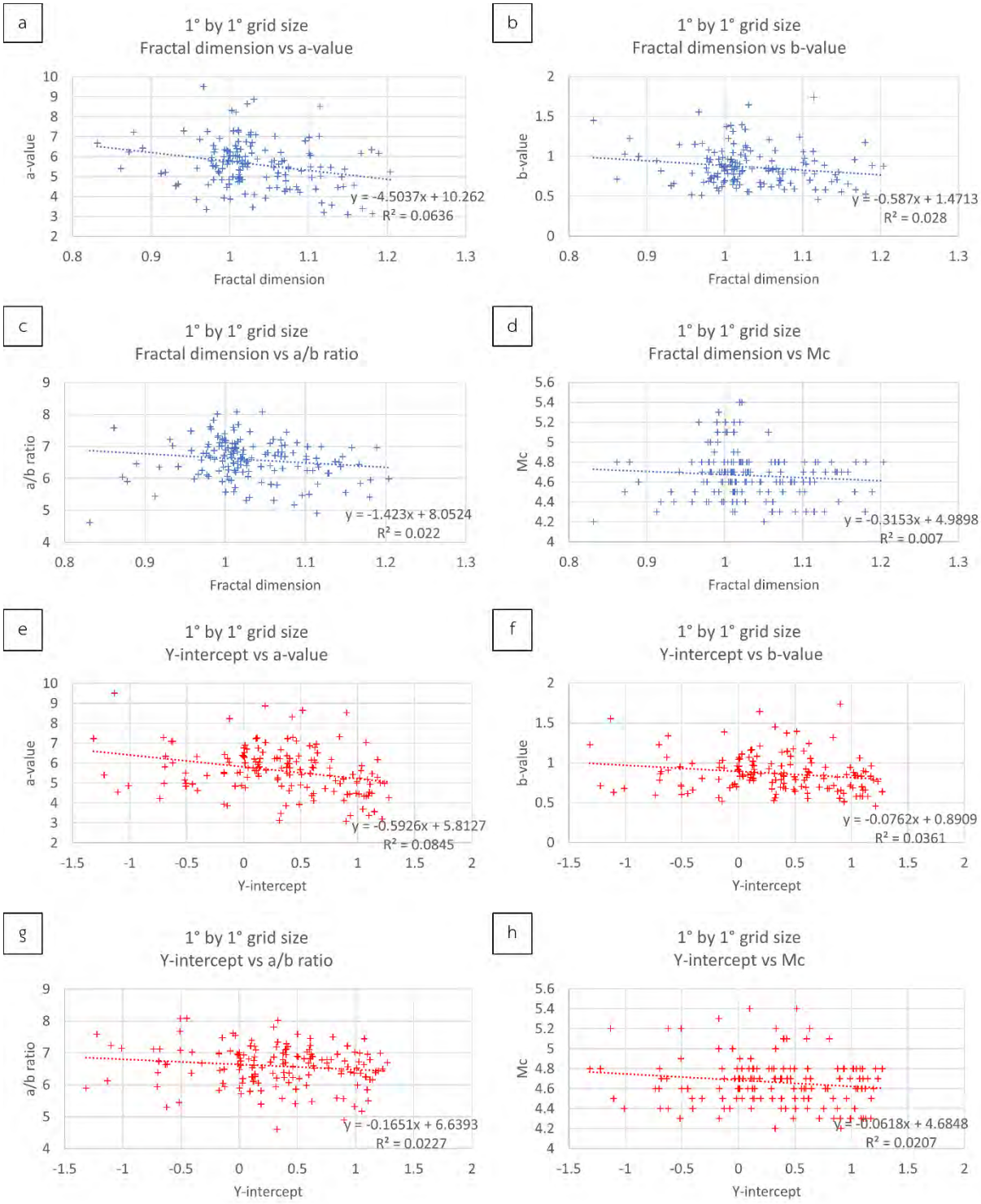

Figure 5.7 Scatter plots representing relationship between values from box-counting method and various seismicity parameters from 1°×1° grid with the total count of 151.

a-d) fractal dimension vs. a-value, b-value, a/b ratio, and magnitude of completeness

e-h) y-axis intercept vs. a-value, b-value, a/b ratio, and magnitude of completeness

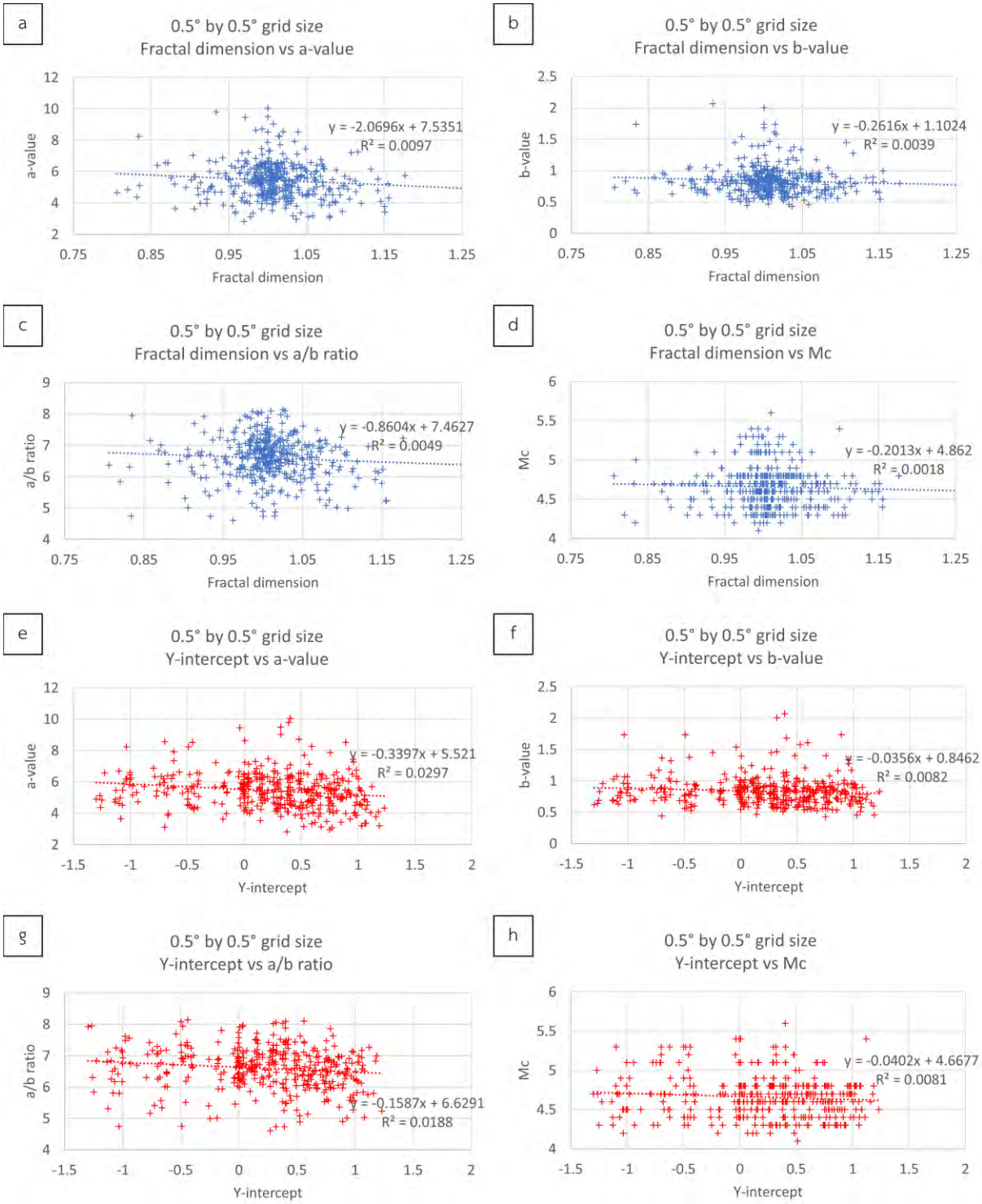

Figure 5.8 Scatter plots representing relationship between values from box-counting method and various seismicity parameters from 0.5°×0.5° grid with the total count of 403.

a-d) fractal dimension vs. a-value, b-value, a/b ratio, and magnitude of completeness

e-h) y-axis intercept vs. a-value, b-value, a/b ratio, and magnitude of completeness

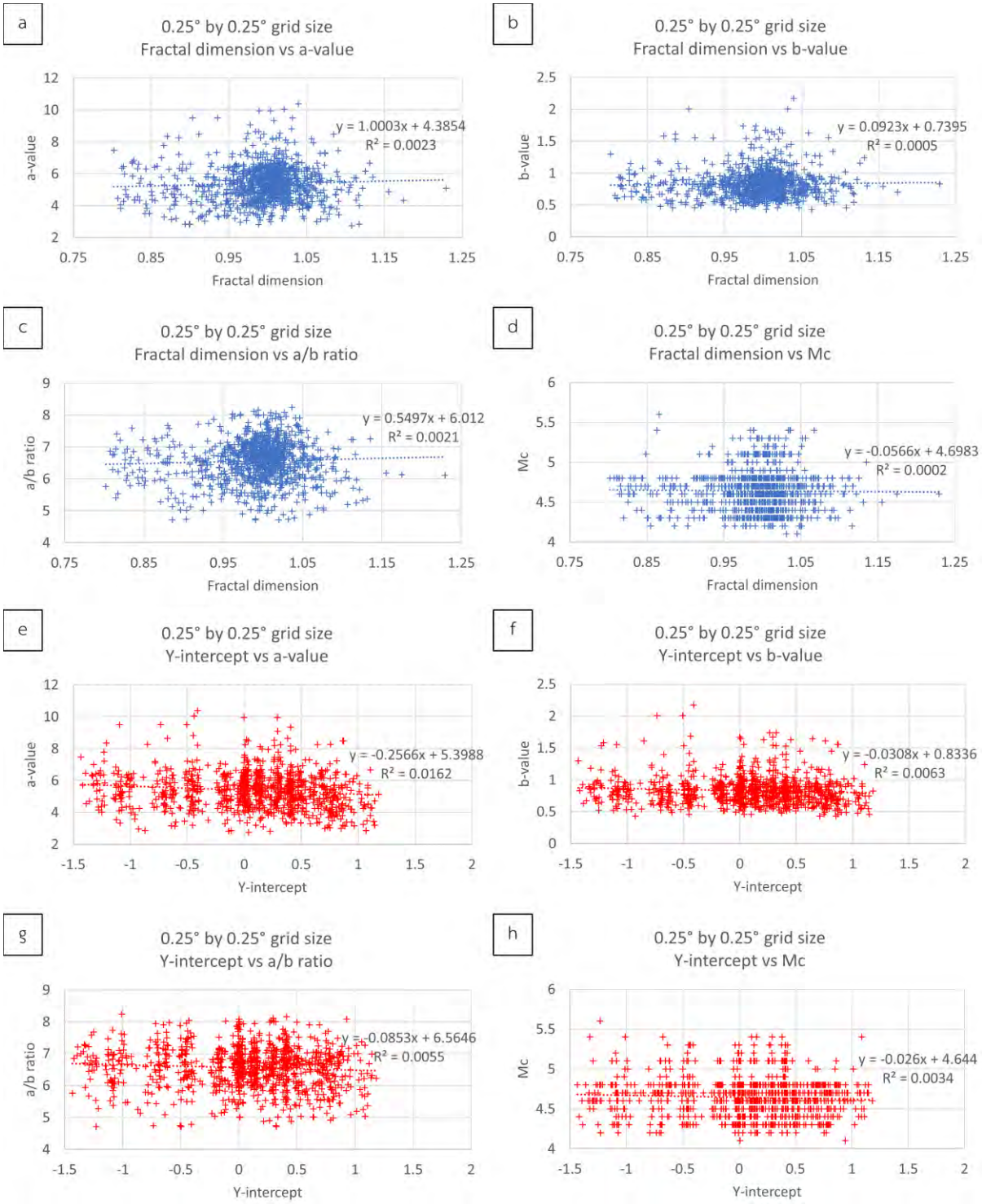

Figure 5.9 Scatter plots representing relationship between values from box-counting method and various seismicity parameters from 0.25°×0.25° grid with the total count of 1,009.

a-d) fractal dimension vs. a-value, b-value, a/b ratio, and magnitude of completeness

e-h) y-axis intercept vs. a-value, b-value, a/b ratio, and magnitude of completeness

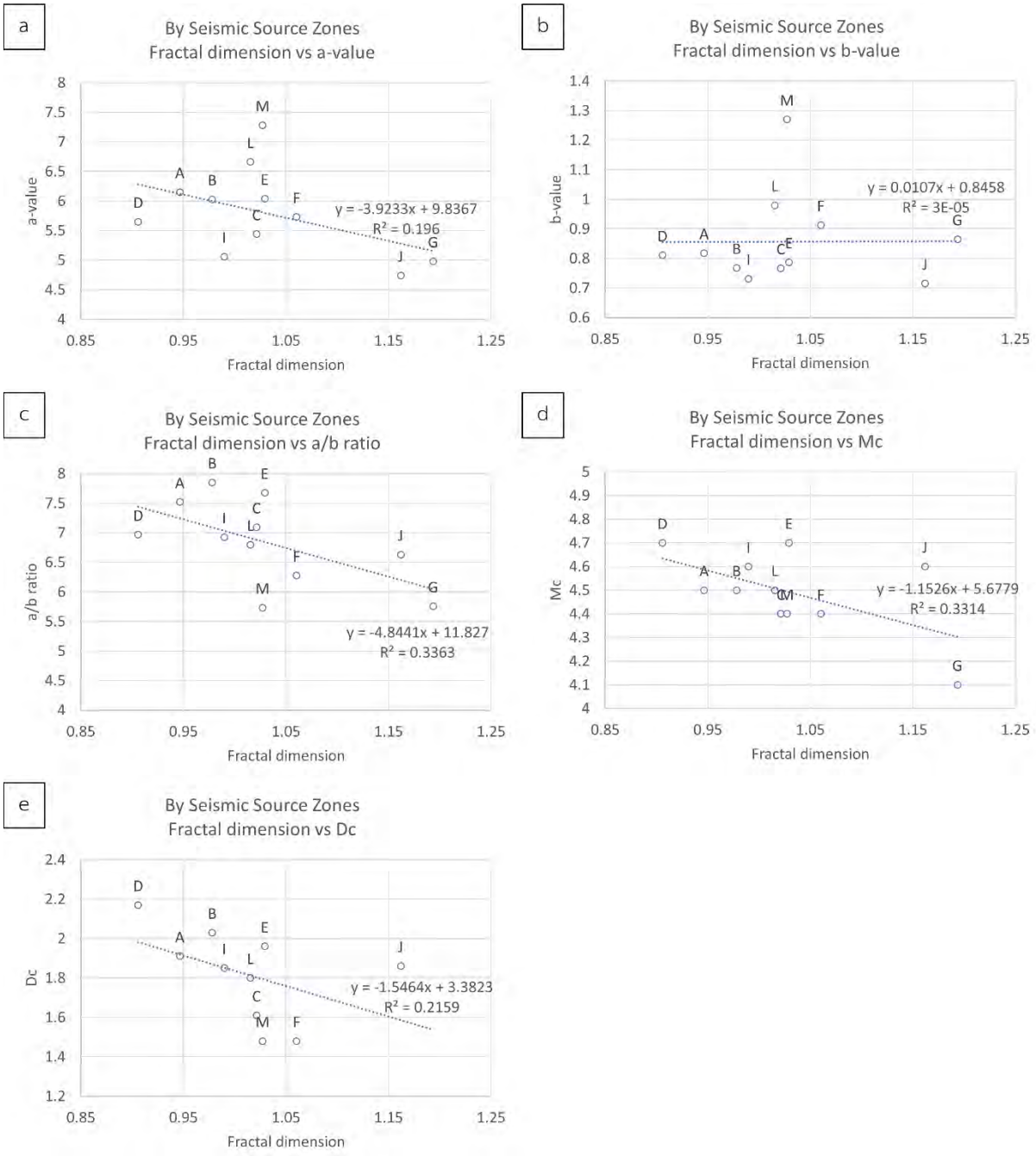

Figure 5.10 Scatter plots representing relationship between fractal dimension and various seismicity parameters based on 13 seismic source zones.

a) a-value

b) b-value

c) a/b ratio

d) magnitude of completeness

e) correlation dimension: D_C (from Pailoplee and Choowong, 2014)

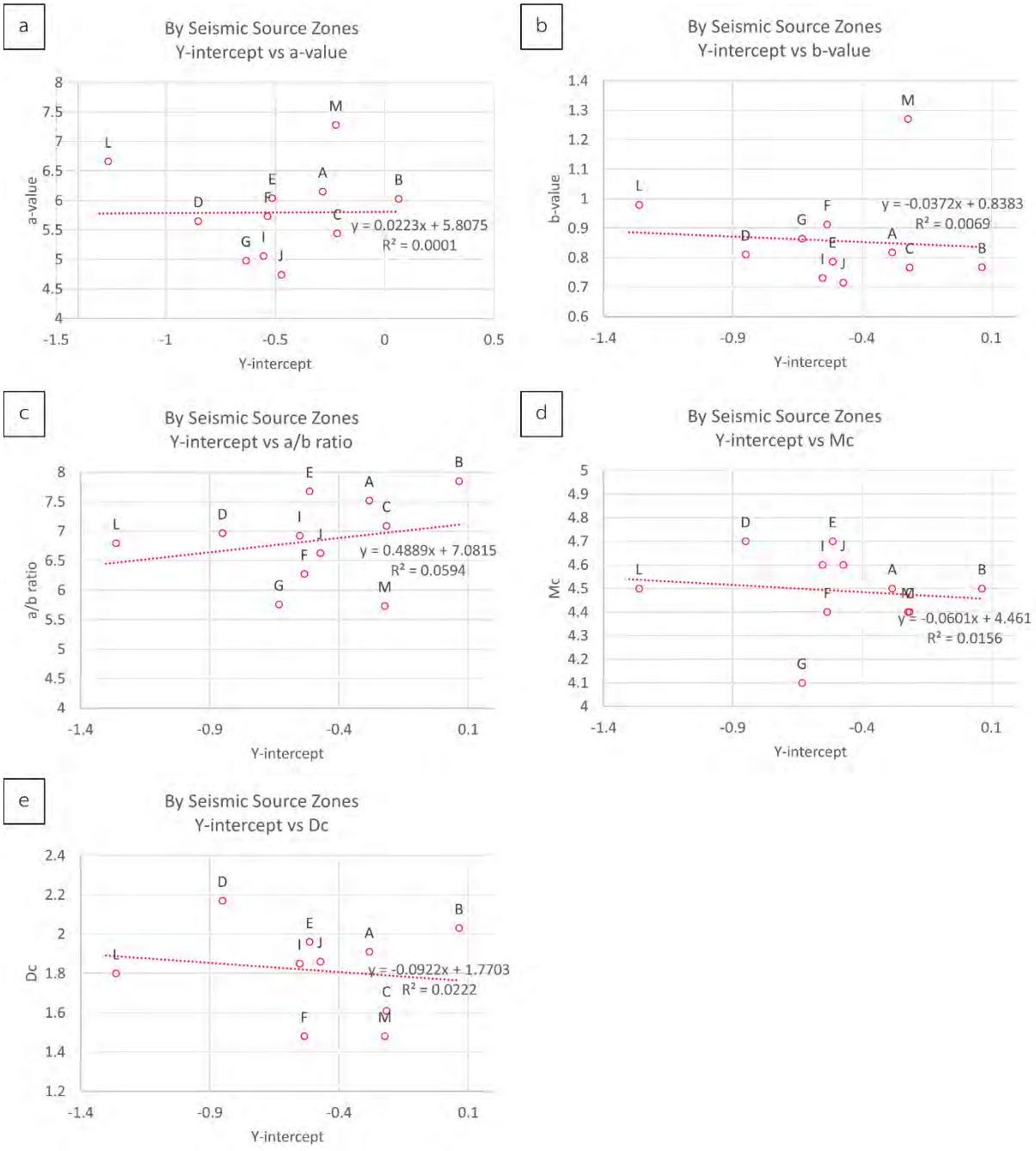

Figure 5.11 Scatter plots representing relationship between y-axis intercept from box-counting plot and various seismicity parameters based on 13 seismic source zones.

a) a-value

b) b-value

c) a/b ratio

d) magnitude of completeness

e) correlation dimension: D_C (from Pailoplee and Choowong, 2014)

5.5. Empirical investigation

As mentioned in previous topics, numerical correlation between fractal dimension and seismicity parameters indicates no direct relationship. However, empirical investigation is also conducted based on comparing fractal dimension anomalies in this study to seismic-prone regions in previous study. Pailoplee (2018) revealed localities in which the b-value is comparatively low indicating high tectonic stress accumulation. These localities are found in the vicinity of complex fault lines as illustrated in fig. This observable evidence may lead to further study in this field.

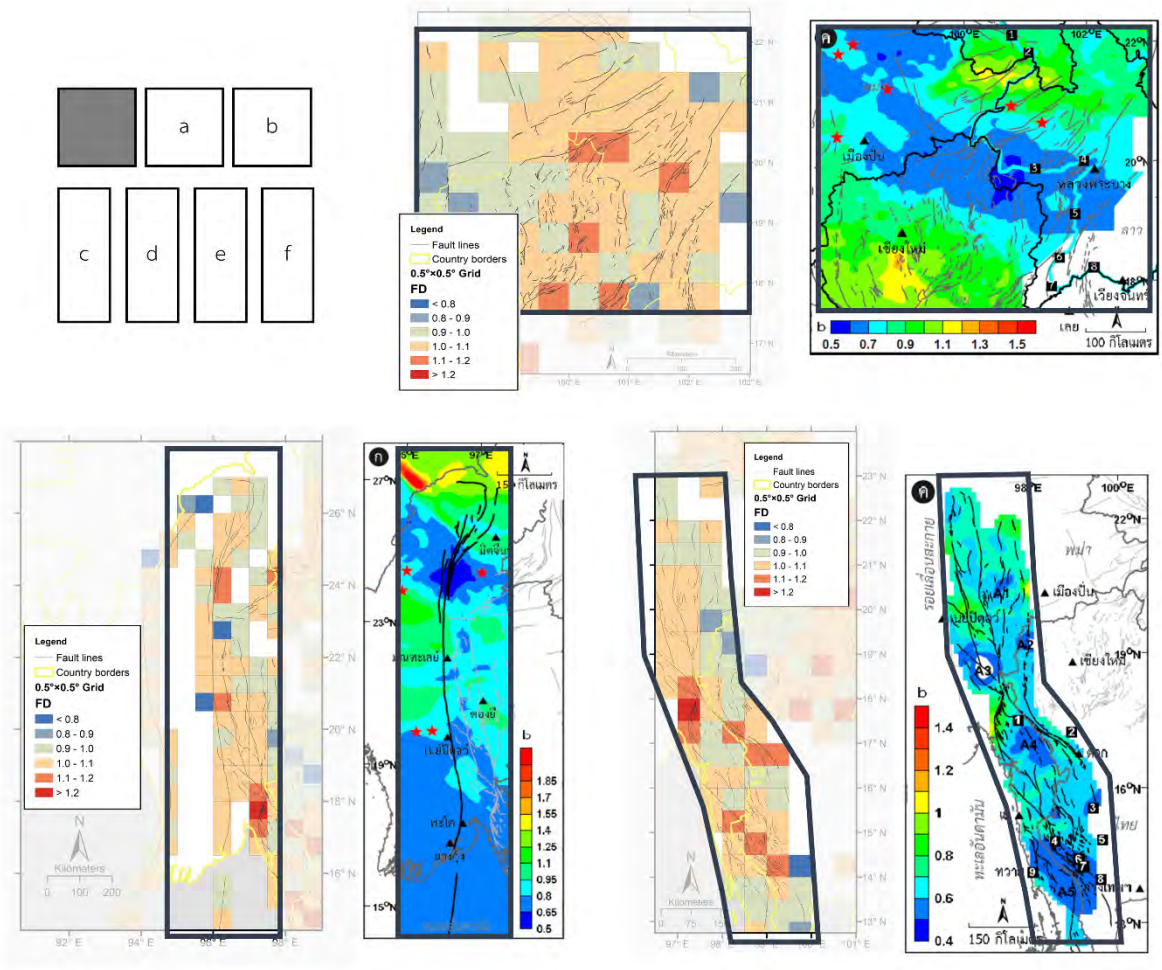

Figure 5.12 Comparison of fractal dimension anomalies (this study) and b-value anomalies (Pailoplee, 2018). a-b) Northern Thailand region. Region along Thailand northern border is the seismic-prone area. c-d) Sagaing Fault Zone. Northern branching of Sagaing Fault is the seismic-prone area. e-f) Western Thailand. Cluster of Three Pagoda, Sri Sawat and Tavoy faults is the seismic-prone area.

5.6. Conclusion

According to the result and discussion mentioned above, the study can be concluded as following. Fractal dimension derived from fault line complexity of the MLSEA ranges from 0.831 to 1.204 in 1°×1° grid size, from 0.806 to 1.253 in 0.5°×0.5° grid size, and from 0.802 to 1.229 in 0.25°×0.25° grid size—excluding those considered outliers. The value of fractal dimension based on the 13 seismic source zones ranges from the lowest of 0.906 in Andaman Basin to the highest of 1.194 in Western Thailand.

Correlating regionally, there is no significant relationship between either fractal dimension or y-axis intercept to any of the seismicity parameters. While correlation based on 13 seismic source zones gives negative linear regression trend in some plots but has no statistical significance as the coefficient of determination (R^2) is very poor. However, empirical investigation unclosed that localities with high fractal dimension match regions of b-value anomaly indicating high tectonic stress.

5.7. Recommendations

Geological fragmentation exhibit fractal characteristics only within a limited range of scale in which the self-similarity exist (Turcotte, 1986). Executing the algorithm in other different grid sizes may emphasis interesting features in the study area.

The original data of fault lines used in this study is a compilation from various researchers, thus, interpretations of fault lines are more or less different from each other. This resulted in non-consistent dataset to work with. For more precise calculation, consistency of fault line interpretation is recommended.

Finally, this method and algorithm of calculating fractal dimension can be used not only in the field of seismology, but also other field related to geology that require a new way of describing complexity, such as crystallography or petrography.

REFERENCES

Anoop, 2011, Finding the Fractal Dimension using Box Counting method.: MATLAB Central File Exchange.

Charusiri, P., Choowong, M., Charoentitirat, T., Jankaew, K., Chutakositkanon, V., and Kanjanapayont, P., 2005, Geological and physical effect evaluation in the tsunami damage area for restoration and warning system: Department of Geology, Faculty of Science, Chulalongkorn University.

Gardner, J. K., and Knopoff, L., 1974, Is the sequence of earthquakes in Southern California, with aftershocks removed, Poissonian? *Bulletin of the Seismological Society of America*, v. 64, no. 5, p. 1363-1367.

Gillespie, P. A., Howard, C. B., Walsh, J. J., and Watterson, J., 1993, Measurement and Characterization of Spatial Distributions of Fractures. *Tectonophysics*, v. 226, no. 1-4, p. 113-141.

Hirata, T., 1989, Fractal Dimension of Fault Systems in Japan - Fractal Structure in Rock Fracture Geometry at Various Scales. *Pure and Applied Geophysics*, v. 131, no. 1-2, p. 157-170.

Lesmoir-Gordon, N., Rood, W., Edney, R., and Appignanesi, R., 2000, Introducing fractal geometry, Duxford, Icon, Introducing, 174 p. p.:

Mandelbrot, B. B., 1983, The fractal geometry of nature, New York, Freeman.

McCaffrey, R., 1996, Slip partitioning at convergent plate boundaries of SE Asia, *in* Hall, R., and Blundell, D., eds., Tectonic Evolution of Southeast Asia The Geological Society, London p. 3-18.

Nutalaya, P., Sodsri, S., and Arnold, E. P., 1985, Series on seismology, Vol. II-Thailand: Southeast Asia Association of Seismology and Earthquake Engineering.

Pailoplee, S., 2018, STATISTICAL SEISMOLOGY: ASEAN Case Study (in Thai), Bangkok, Chulalongkorn University Book Center, 660 p.:

Pailoplee, S., and Charusiri, P., 2016, Seismic hazards in Thailand: a compilation and updated probabilistic analysis. *Earth Planets and Space*, v. 68.

Pailoplee, S., and Choowong, M., 2013, Probabilities of earthquake occurrences in Mainland Southeast Asia. *Arabian Journal of Geosciences*, v. 6, no. 12, p. 4993-5006.

Pailoplee, S., and Choowong, M., 2014, Earthquake frequency-magnitude distribution and fractal dimension in mainland Southeast Asia. *Earth Planets and Space*, v. 66.

Pailoplee, S., Sugiyama, Y., and Charusiri, P., 2009, Deterministic and probabilistic seismic hazard analyses in Thailand and adjacent areas using active fault data. *Earth Planets and Space*, v. 61, no. 12, p. 1313-1325.

Pailoplee, S., Sugiyama, Y., and Charusiri, P., 2010, Probabilistic Seismic Hazard Analysis in Thailand and Adjacent Areas by Using Regional Seismic Source Zones. *Terrestrial Atmospheric and Oceanic Sciences*, v. 21, no. 5, p. 757-766.

Poolachan, S., and Satayarak, N., Strike-slip tectonics and the development of Tertiary basins in Thailand, in *Proceedings Proceedings of the International Symposium on Intermontane Basin: Geology and Resources*, Chiang Mai, Thailand, 30 Jan-2 Feb 1989 1989, p. 243-253.

Sarp, G., 2014, Evolution of neotectonic activity of East Anatolian Fault System (EAFS) in Bingol pull-apart basin, based on fractal dimension and morphometric indices. *Journal of Asian Earth Sciences*, v. 88, p. 168-177.

Schroeder, M., 1991, Fractals, Chaos, Power Laws: Minutes from an Infinite Paradise, New York, Dover Publications Inc., 448 p.:

Sengupta, P., Nath, S. K., Thingbaijam, K. K. S., and Mistri, S., 2011, Fractal analysis of major faults in India on a regional scale. *Journal of the Geological Society of India*, v. 78, no. 3, p. 226-232.

Tapponnier, P., Peltzer, G., Le Dain, A. Y., Armijo, R., and Cobbold, P., 1982, Propagating extrusion tectonics in Asia: New insights from simple experiments with plasticine. *Geology*, v. 10, no. 12, p. 611-616.

Turcotte, D. L., 1986, Fractals and Fragmentation. *Journal of Geophysical Research*, v. 91, p. 1921 -1926.